



HAL
open science

Regulation of YAP by mTOR and autophagy reveals a therapeutic target of Tuberous Sclerosis Complex

Ning Liang

► **To cite this version:**

Ning Liang. Regulation of YAP by mTOR and autophagy reveals a therapeutic target of Tuberous Sclerosis Complex. Cellular Biology. Université René Descartes - Paris V, 2014. English. NNT : 2014PA05T055 . tel-01126889

HAL Id: tel-01126889

<https://theses.hal.science/tel-01126889>

Submitted on 6 Mar 2015

HAL is a multi-disciplinary open access archive for the deposit and dissemination of scientific research documents, whether they are published or not. The documents may come from teaching and research institutions in France or abroad, or from public or private research centers.

L'archive ouverte pluridisciplinaire **HAL**, est destinée au dépôt et à la diffusion de documents scientifiques de niveau recherche, publiés ou non, émanant des établissements d'enseignement et de recherche français ou étrangers, des laboratoires publics ou privés.

**UNIVERSITE PARIS DESCARTES
FACULTE DE MEDECINE PARIS DESCARTES**

THESE
Pour obtenir le grade de
DOCTEUR DE L'UNIVERSITE PARIS DESCARTES

Spécialité
Biologie cellulaire

**Regulation of YAP by mTOR and autophagy reveals
a therapeutic target of Tuberous Sclerosis Complex**

Présentée par
Ning LIANG

Directeur de thèse
Dr. Mario PENDE

Soutenue le 29 Septembre 2014

Membres du jury :

Le Dr. Bertrand Knebelmann
Le Dr. Richard Lamb
Le Dr. Hugo Stocker
Le Dr. Mario Pende

Président
Rapporteur
Rapporteur
Directeur de thèse

Summary

The Tuberous Sclerosis Complex (TSC) is a genetic disease characterized by growth of hamartomas in different organs including brain, kidney, lung, skin, and heart. These lesions are sources of morbidity and mortality in patients with TSC, as they may cause intractable epilepsy, autism, developmental delay, renal and pulmonary failure. Known causes of TSC are loss of function mutations in TSC1 and TSC2 genes. The majority of TSC lesions contain multiple cell types of the mesenchymal lineage, as in the case of angiomyolipomas, lymphangiomyomatosis and angiofibromas. A unique cell type named perivascular epithelioid cell (PEC) is constantly present in mesenchymal TSC lesions, such as angiomyolipomas and lymphangiomyomatosis, basing on morphological features and the common expression of melanocytic and myogenic markers. Therefore, these lesions are officially classified, along with other tumors, as PEComas. Their cell of origin and the molecular mechanisms underlying their pathogenesis remain poorly defined.

Here we generated a novel mosaic *Tsc1* knockout mouse model which develops renal mesenchymal lesions recapitulating human Perivascular Epithelioid Cell tumor (PEComa) observed in TSC patients. We identified YAP, the transcriptional coactivator of Hippo pathway, was upregulated in both renal lesions of TSC mouse model and human angiomyolipoma samples in a mTOR-dependent manner. Inhibition of YAP with genetic or pharmacological tools greatly attenuates the proliferation and survival of *Tsc1* null cells *in vivo* and *in vitro*. Furthermore, we found YAP accumulation in TSC1/TSC2 deficient cells is due to impaired degradation of the protein through the autophagosome/lysosome system.

Thus the regulation of YAP by mTOR and autophagy is a novel mechanism of growth control, matching YAP activity with nutrient availability under growth permissive conditions. It may serve as a potential therapeutical target for TSC and other diseases with dysregulated mTOR activity.

Abbreviation

AML	Angiomyolipoma
AMP	Adenosine monophosphate
Areg	Amphiregulin
ATP	Adenosine triphosphate
ATG7	Autophagy-related protein 7
BrdU	5-Bromo-2-deoxyuridine
CQ	Chloroquine
CTGF	Connective tissue growth factor
4E-BP1	Eukaryotic initiation factor 4E binding protein 1
GAP	GTPase activating protein
GEF	Guanine nucleotide exchange factor
GTP	Guanosine triphosphate
GTPase	Guanosine triphosphatase
HEK293	Human embryonic kidney cell 293
LAM	Lymphangioliomyomatosis
Lats1/2	large tumor suppressor, homolog 1/2
MEF	Mouse embryonic fibroblast
MST1/2	mammalian Sterile20-like 1/2
mTOR	mammalian (mechanistic) target of rapamycin
mTORC1	mammalian (mechanistic) target of rapamycin complex1
mTORC2	mammalian (mechanistic) target of rapamycin complex2
PEComa	Perivascular epithelioid cell tumor
PI3K	Phosphatidylinositol-3 Kinase
PI3P	Phosphatidylinositol-3-phosphate

PTEN	Phosphatase and tensin homolog on chromosome 10
Raptor	Regulatory associated protein of mTOR
Rheb	Ras homolog enriched in brain
Rictor	Rapamycin-insensitive companion of mTOR
rpS6	Ribosomal protein S6
SEGA	Subependymal giant cell astrocytomas
S6K	Ribosomal protein S6 kinase
S6K1	Ribosomal protein S6 kinase 1
S6K2	Ribosomal protein S6 kinase 2
TUNEL	Terminal deoxyribonucleotidyl transferase (TDT)-mediated dUTP-digoxigenin nick end labeling
TSC	Tuberous sclerosis complex
TSC1	Tuberous sclerosis complex 1 (hamartine)
TSC2	Tuberous sclerosis complex 2 (tuberine)
TBC1D7	TBC1 domain family, member 7
Vps15	Vacuolar Protein Sorting 15
YAP	Yes associated protein

1.2.3	Regulation of YAP/TAZ in mammals	22
1.2.3.1	Phosphorylation-dependent cytoplasmic sequestration	22
1.2.3.2	Phosphorylation-dependent degradation through ubiquitin-proteasome pathway	22
1.2.3.3	Phosphorylation-independent regulation.....	22
1.2.4	Crosstalk between two master regulators of organ size, mTOR signaling and Hippo-YAP signaling.....	23
2	Results.....	24
2.1	Generation of mosaic- <i>Tsc1</i> KO mice which develop multisystem lesions showing similarities with human TSC.....	24
2.2	Mosaic- <i>Tsc1</i> KO mice develop renal mesenchymal lesions recapitulating PEComas associated with human TSC.	26
2.3	YAP is up-regulated by mTOR in renal lesions of mosaic- <i>Tsc1</i> KO mice and human angiomyolipoma.....	30
2.4	YAP is required for the abnormal proliferation and survival of TSC1/2 null cells <i>in vitro</i>	34
2.5	Inhibition of YAP pharmacologically or genetically attenuates abnormal proliferation and induces apoptosis of <i>Tsc1</i> null cells <i>in vivo</i>	37
2.6	YAP is accumulated in TSC deficient cells due to blockage of autophagy in a mTOR-dependent manner.	41
3	Conclusion and discussion.....	46
3.1	The cell of origin of TSC-associated PEComas	46
3.1.1	Pericytes.....	46
3.1.2	Smooth muscle cells.....	47
3.1.3	Neural crest cells	47
3.2	Potential pharmacological strategies against YAP for TSC lesions	47
3.2.1	GPCR agonist/antagonist.....	48
3.2.2	Statins	48
3.2.3	Peptides inhibiting interaction between YAP and TEAD.....	49
3.3	Regulation of YAP degradation by autophagy	49
4	Materials and Methods.....	52
5	References	57
6	Publication	72
7	Acknowledgements.....	73

1 Introduction

1.1 Tuberous Sclerosis Complex

Tuberous Sclerosis Complex (TSC) is a human genetic disease which is characterized by development of hamartomas in multiple organs including brain, kidney, lung, skin and heart. These benign tumors lead to a combination of symptoms such as seizures, developmental delay, autism, skin abnormality, renal and pulmonary failure. TSC is caused by loss of function mutations in two genes, *TSC1* (9q34) and *TSC2* (16p13). The prevalence of TSC is estimated to be 1 in 6,000 individuals (Crino et al., 2006).

1.1.1 Clinical features

1.1.1.1 Brain

TSC patients can be affected by three types of tumors in the brain: cortical tuber, subependymal nodules, subependymal giant cell astrocytomas (SEGA). 80% of TSC patients develop cortical tubers, which is a developmental abnormality characterized by neuronal dys-lamination, dysmorphic neurons and enlarged astrocytes in the cortex. Subependymal nodules form along the walls of lateral and third ventricles featured by abnormal glial cells and multinucleated cells. SEGA are composed of proliferative astrocytes and giant cells which usually arise near foramen of Monro, channels connecting lateral and third ventricles.

1.1.1.2 Kidney

55% to 75% of TSC patients develop renal angiomyolipomas (AML) which are composed of abnormal blood vessels, smooth muscle cells and adipocytes. Their

occurrence are usually bilateral and multiple. Angiomyolipomas may cause spontaneous bleeding and hemorrhages when their size is larger than 3 cm in diameter. Another morbidity associated with angiomyolipomas is the chronic kidney disease and renal failure caused by progressive infiltration of angiomyolipomas in some cases.

Although the classic angiomyolipomas contain three components including abnormal vasculatures, proliferative smooth muscle cells and fat cells, the contribution of each part can be viable from case to case. In some patients, the angiomyolipomas are composed of mainly smooth muscle cells and vasculatures, thus named fat poor angiomyolipomas; while in other cases, adipocytes could be the dominate component. Through genetic studies, similar second-hit mutations were identified in all the three components from the same angiomyolipoma sample indicating they are derived from one progenitor cell (El-Hashemite et al., 2003; Karbowniczek et al., 2003). However, the cell of origin of angiomyolipomas remains elusive.

A distinctive cell type, perivascular epithelioid cell (PEC), is constantly found in angiomyolipomas, because of which angiomyolipomas are classified as PEComas (discussed below). Intriguingly, Perivascular epithelioid cells express both melanocytic (Hmb45 and/or Mart1) and myogenic (α SMA) markers, while its normal tissue counterpart is not yet identified. Since melanocyte is derived from neural crest during vertebrate development, it is postulated that PEComas are originated from neural crest cells (Sarnat and Flores-Sarnat, 2005). Because angiomyolipomas are mesenchymal and the epithelial cells of kidneys are generated from embryonic mesoderm, it is also hypothesized that angiomyolipomas arise from abnormal mesenchymal-epithelial transition during early kidney development or aberrant epithelial-mesenchymal transition occurred in TSC1/2 null renal tubular cells during late kidney developmental stages. These different possibilities still need to be tested to identify the cell of origin of angiomyolipomas.

Epithelial lesions, such as cysts and renal cell carcinomas, are also associated with TSC with relatively low incidences of 20-30% and 2-3% respectively.

1.1.1.3 Lung

Lymphangiomyomatosis (LAM) are female-dominant pulmonary tumors associated with TSC which affect 26-39% of female patients. They are composed of proliferative smooth muscle cells which could infiltrate different pulmonary structures, such as airways, alveolar septa and vasculatures. Similar with angiomyolipomas, perivascular epithelioid cells are also identified in lymphangiomyomatosis, which express both melanocytic and myogenic markers. Around 30-60% patients with sporadic LAM were also affected with angiomyolipomas. Interestingly, the same mutated loci were identified both in LAM cells and in angiomyolipomas cells from the same patients indicating they may arise from the same ancestor or LAM may be a result of metastasis of mesenchymal cells from renal angiomyolipomas or *vice versa* (Carsillo et al., 2000). However, this hypothesis remains to be tested experimentally.

1.1.1.4 Skin

Dermatological symptoms are present in 90% of TSC patients including facial angiofibromas, periungual fibromas and hypomelanotic macules. They are among the major diagnostic criteria of TSC and usually cause no problems.

1.1.1.5 Heart

Cardiac rhabdomyomas are associated with 50-70% TSC infants. A few of them may cause significant clinical problems. They usually disappear spontaneously in later adult life of the patients.

1.1.1.6 Perivascular Epithelioid Cell tumors (PEComas)

Most of the tumors associated with TSC are mesenchymal, such as angiomyolipomas, lymphangiomyomatosis, angiofibromas and rhabdomyomas. In renal angiomyolipomas and pulmonary lymphangiomyomatosis, a unique cell

type, perivascular epithelioid cell (PEC), is constantly present in these tumors, because of which these tumor are classified as PEComas (Martignoni et al., 2008; Pea et al., 1996). Morphologically, PEC has epithelioid appearance characterized by clear to granular cytoplasm and round to oval central-located nuclei. They are usually located near vasculatures. Immunohistochemically, PEC shows expression of both myogenic and melanocytic markers. The cell of origin of these tumors remains elusive and the molecular mechanism governing their initiation and progression is yet to be fully defined.

1.1.2 Genetics

Two TSC-determining genetic loci, *TSC1* and *TSC2*, were identified by linkage analysis and positional cloning utilizing multigenerational family samples (Kandt et al., 1992; van Slegtenhorst et al., 1997). *TSC1* is located on chromosome 9q34 and *TSC2* is located on chromosome 16p13. A wide spectrum of mutations were found in these two genes of TSC patients including allelic variants, missense mutations and large genomic deletions. In some cases, large genomic deletions in *TSC2* also disrupt the adjacent *PKD1* causing severe polycystic kidney disease.

The frequency of mutations in these two genes are different. Mutations in *TSC1* were mapped in 15% of TSC patients, while *TSC2* mutation were identified in 80-90% of TSC patients. Loss of heterozygosity (LOH) in these two genes were found in the majority of TSC associated tumors, indicating *TSC1* and *TSC2* are tumor suppressor genes according to Knudson's two-hit model (Knudson, 1971; Sepp et al., 1996).

1.1.3 Pathophysiology

1.1.3.1 TSC1 and TSC2, one protein complex

TSC1 encodes a 140 kDa protein which shows no homology with other proteins. The 200 kDa *TSC2* protein was identified to harbor a GTPase activating protein (GAP)

domain in its C-terminal region (Wienecke et al., 1995; Xiao et al., 1997). This domain was found to be responsible for the tumor suppressor activity of TSC2 using cell culture and xenograft experiments (Jin et al., 1996). Both of these two proteins are evolutionally conserved from yeast to human.

A functional link between TSC1 and TSC2 proteins was established in later studies which demonstrated that these two proteins are physically associated with each other (Plank et al., 1998; van Slegtenhorst et al., 1998). TSC1 is essential in stabilizing TSC2 protein and preventing its degradation by ubiquitin-proteasome pathway (Benvenuto et al., 2000). The interdependent property of this heterodimeric protein complex were further validated in fruitfly and yeast (Gao and Pan, 2001; Matsumoto et al., 2002; Potter et al., 2001).

1.1.3.2 TSC1/TSC2 complex, a tumor suppressor in Insulin signaling pathway

Loss of function mutations of *Tsc1* or *Tsc2* in *Drosophila* led to massive tissue overgrowth which was characterized by increased cell proliferation and enlarged cell size. The phenotype of *Tsc1-Tsc2* double mutant was similar to either *Tsc1* or *Tsc2* single mutant. In addition, overexpression of either *Tsc1* or *Tsc2* alone had no effect on tissue growth, while overexpression of both of them dramatically attenuated organ size through decreased cell proliferation and cell size. These observations implicated that *Tsc1* and *Tsc2* function together as a tumor suppressor regulating both cell proliferation and cell size during tissue growth (Gao and Pan, 2001; Tapon et al., 2001).

Insulin signaling was previously identified to be an important regulator of tissue growth during development in *Drosophila* (Stocker and Hafen, 2000). *Tsc1* or *Tsc2* mutant fruit flies showed similar phenotypes with *Pten* (phosphatase and tensin homologue deleted on chromosome 10) mutant, a negative regulator in insulin signaling (Gao et al., 2000; Goberdhan et al., 1999; Huang et al., 1999). Overexpression of insulin receptor led to lethality in *Drosophila* and this could be rescued by co-overexpression of *Tsc1* and *Tsc2* but not by overexpression of either

Tsc1 or *Tsc2* alone. Through extensive genetic epistasis studies in *Drosophila*, TSC1/TSC2 complex was positioned in insulin signaling pathway downstream of Insulin Receptor/PTEN/AKT (protein kinase B) and upstream of S6K (ribosomal protein S6 kinase) by 2001 (Potter et al., 2001).

1.1.3.3 TSC1/TSC2 complex, an inhibitor of mTOR through Rheb

Subsequent studies in *Drosophila* showed that the phenotypes of *Tsc1* or *Tsc2* mutants could be rescued by deletion of an upstream activator of S6K, TOR (target of rapamycin) which was later known to be a core kinase in insulin signaling pathway and master regulator of cell growth and metabolism (Gao et al., 2002). Inhibition of mTOR (mammalian target of rapamycin) by rapamycin induced apoptosis and suppressed proliferation of TSC1 or TSC2 null cells in vitro and in mice (Kenerson et al., 2002).

Furthermore, a small G-protein Rheb (Ras homologue enriched in brain) was identified linking TSC1/TSC2 complex to mTOR. In *Drosophila*, Rheb was identified to be a positive regulator of tissue growth upstream of TOR and S6K, downstream of TSC1/TSC2 complex (Stocker et al., 2003). Biochemical studies showed that TSC1/TSC2 complex could directly bind and inhibit Rheb GTPase activity through the GAP domain of TSC2 (Inoki et al., 2003). GTP-bound thus activated Rheb could directly bind and activate mTOR kinase activity (Long et al., 2005).

Thus, TSC1/TSC2 complex was identified to be a tumor suppressor through inhibiting mTOR activity.

1.1.3.4 TSC1/2-mTORC1 signaling

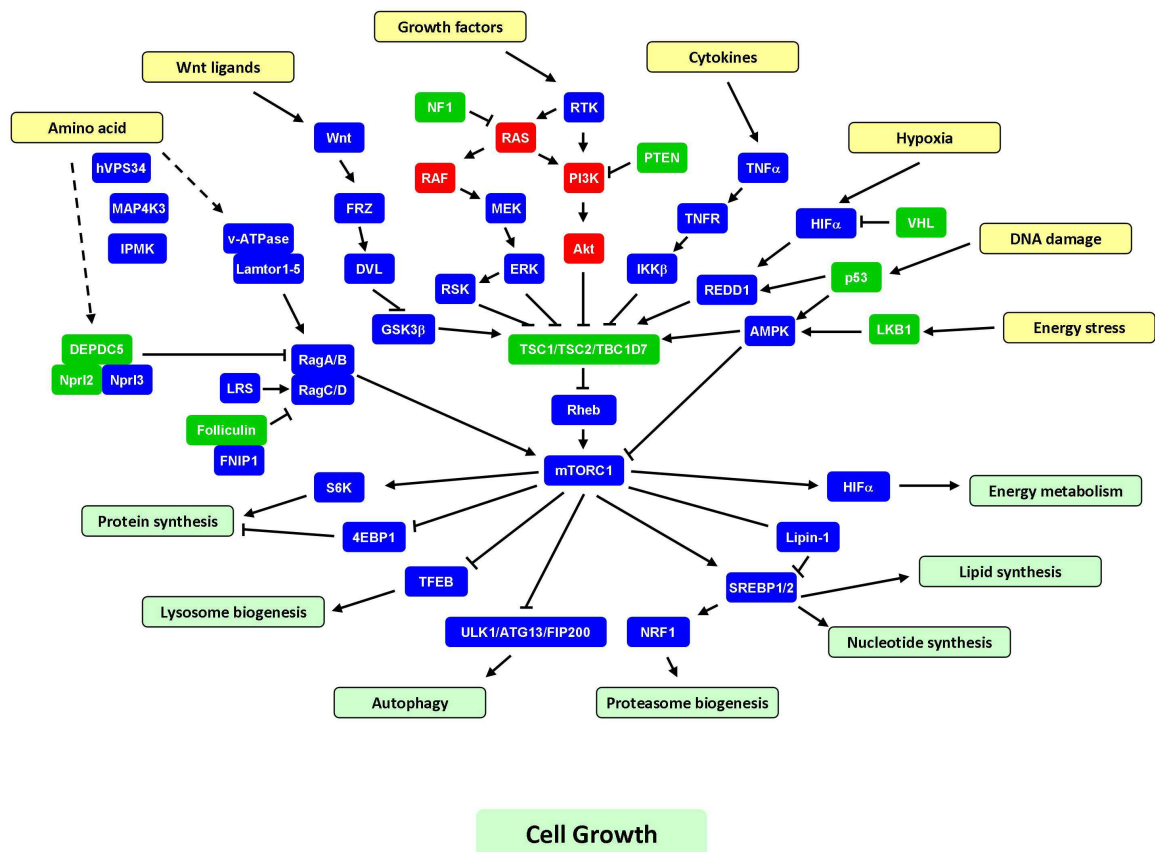


Figure 1. TSC1/TSC2/TBC1D7-mTORC1 signaling pathway.

mTOR kinase functions in two distinct complexes regulating cell proliferation, survival and cell metabolism (Laplante and Sabatini, 2012). mTOR kinase complex 1 (mTORC1) is composed of mTOR, raptor (regulatory associated protein of mTOR), LST8 (lethal with SEC13 protein 8), PRAS40 (proline-rich Akt substrate 40 kDa), DEPTOR (DEP domain containing mTOR-interacting protein) and Tti/Tel2 complex while mTOR kinase complex 2 (mTORC2) consists of mTOR, rictor (rapamycin-insensitive companion of mTOR), SIN1 (stress-activated protein kinase interacting protein 1), LST8, DEPTOR and Tti/Tel2. The primary role of TSC1/TSC2 complex is a negative regulator of mTORC1 through inhibition of Rheb activity.

TSC1/2-mTORC1 pathway senses and integrates a diversity of upstream signals including growth factors, amino acids, oxygen, energy status and stress to control cell growth (Huang and Manning, 2008).

Growth factors activates mTORC1 through PI3K/Akt/TSC1-TSC2/Rheb signaling axis. TSC2 is phosphorylated by Akt primarily on Serine939 and Theronine1462 in response to growth factor stimulation (Inoki et al., 2002). Although this phosphorylation event do inhibit the activity of TSC1/TSC2 complex toward Rheb/mTORC1, the GAP activity of TSC2 is not altered upon phosphorylation by Akt. By cellular fractionation studies, it was reported that more TSC2 was detected in the cytosolic fractions rather than membrane fractions following growth factor stimulation (Cai et al., 2006). TSC1/TSC2 complex is later identified to detach from lysosomes and lose contact with Rheb, a portion of which is residing on the surface of lysosomes and activating mTORC1 there, upon phosphorylation by Akt in response to growth factors (Menon et al., 2014). In addition, ERK and RSK are also demonstrated to directly phosphorylate TSC2 and promote mTORC1 activation in response to growth factor treatment (Roux et al., 2004).

Inflammatory cytokine tumor necrosis factor α (TNF α) activates mTORC1 signaling through TSC1. It was uncovered that the downstream kinase of TNF α signaling inhibitory κ B kinase β (IKK β) bind and phosphorylate TSC1 on Serine487 and Serine511, leading to disruption of TSC1/TSC2 complex and degradation of TSC1 (Lee et al., 2007).

Cellular energy stress, such as accumulation of AMP, rapidly inhibit mTORC1 activity through LKB1 (Liver kinase B1)/AMPK (AMP-dependent protein kinase) signaling pathway (Shaw et al., 2004). Activated AMPK phosphorylates and activates TSC2 on Threonine1271 and Serine1387. Low oxygen levels also lead to mTORC1 inactivation through transcriptional activation of REDD1 (regulated in DNA damage and development 1) by HIF α (Brugarolas et al., 2004). REDD1 triggers the dephosphorylation and activation of TSC2 through removal of 14-3-3 proteins associated Serine939 and Theronine1462 and PP2A-dependent dephosphorylation of Akt on Thr308 (but not Ser473) (Dennis et al., 2014). DNA damage inhibits mTORC1 signaling by activating TSC1/TSC2 complex through both AMPK and REDD1 (Corradetti et al., 2004). In addition, Wnt signaling has been shown to

activate mTORC1 signaling by glycogen synthesis kinase 3 β (GSK3 β)-mediated phosphorylation of TSC2 (Inoki et al., 2006; Mak et al., 2005).

Amino acids availability tightly regulates mTORC1 activity. It is mainly through heterodimeric GTPases RagA/B and RagC/D, which were anchored to lysosomes through Ragulator protein complex (Lamtor1-5) and v-ATPase (Sancak et al., 2010; Sancak et al., 2008; Zoncu et al., 2011). With high amino acids levels, RagA/B is charged with GTP and RagC/D is bound to GDP, which facilitate mTORC1 lysosomal localization and activation. Several protein complex, such as GATOR1 (DEPC5, Nprl2, Nprl3), GATOR2 (Mios, Seh1l, WDR24, WDR59, Sec13) and Folliculin complex (Folliculin and FNIP1) which have GAP or GEF activities toward Rag GTPase, are identified to be involved in the activation of mTORC1 by amino acids (Bar-Peled et al., 2013; Bar-Peled et al., 2012). In addition, the class III PI3K vacuolar protein sorting 34 (VPS34), the Ste20 related kinase mitogen-activated protein kinase kinase kinase kinase 3 (MAP4K3) and inositol polyphosphate multikinase (IPMK) are linked to mTORC1 signaling activation by amino acids (Byfield et al., 2005; Findlay et al., 2007; Kim et al., 2011). Whether TSC1/TSC2 complex is involved in the amino acid-induced mTORC1 activation remains to be fully understood. In TSC2 null cells, amino acid withdraw leads to more than 50% decrease of mTORC1 signaling measured by phosphorylation of its downstream targets S6K and 4EBP1 (Smith et al., 2005), indicating that there are amino acids sensing pathways leading to mTORC1 activation independent of TSC1/TSC2 complex. It has been shown recently that upon amino acid withdraw, Rag GTPases release mTORC1 from lysosome surface and recruit TSC1/TSC2 to the lysosome to inhibit Rheb in the mean time. Without TSC2, cells can not fully release mTORC1 from lysosome (Demetriades et al., 2014). This may partially explain the residue mTORC1 activity upon amino acid removal in TSC2 null cells. However, the direct molecular sensor of amino acids remain to be identified.

By phosphorylating specific effector proteins, mTORC1 regulates multiple downstream signaling pathways. mTORC1 promotes protein synthesis by phosphorylating S6 kinase 1 (S6K1) and translational regulators eukaryotic translation initiation factor 4E binding protein 1 (4E-BP1) (Laplante and Sabatini, 2012). mTORC1 directly phosphorylates Lipin1, leading to its cytoplasmic

sequestration and facilitating sterol regulatory element-binding protein 1/2 (SREBP1/2) function, to drive nucleotides, lipid synthesis and proteasome biogenesis (Peterson et al., 2011; Zhang et al., 2014b). mTORC1 regulates energy metabolism through activating the transcription and translation of hypoxia inducible factor 1 α (HIF1 α). Through phosphorylating and inhibiting TFEB nuclear translocation, mTORC1 suppresses lysosome biogenesis (Settembre et al., 2012). mTORC1 also directly phosphorylates a kinase complex, consisting of ULK1/Atg13/FIP200 (unc-51-like kinase 1/ mammalian autophagy-related gene 13/ focal adhesion kinase family-interacting protein of 200 kDa), to inhibit the initiation of autophagy, which is an eukaryotic catabolic pathway that sequesters cellular organelles and proteins in double-membrane autophagosomes, delivers and degrades the cargos in lysosomes (Xie and Klionsky, 2007).

1.1.3.5 TSC1 and TSC2 function beyond mTORC1

Although TSC1 and TSC2 have been shown to function in one complex inhibiting mTORC1 signaling pathway, it does not rule out the possibility that they may also function separately and independent of mTORC1. TSC1 was identified to interact with actin binding protein ezrin-radixin-moesin. Cells which are deficient of TSC1 showed decreased focal adhesion formation. Overexpression of TSC1 led to activation of small GTPase Rho which induced stress fiber assembly and focal adhesion formation (Lamb et al., 2000). Furthermore, overexpression of TSC2 also activated GTPase Rho, but not Rac1 or cdc42, through which regulating cell adhesion and migration (Astrinidis et al., 2002).

TSC1/TSC2 was demonstrated to interact with and promote the activity of mTORC2. In TSC1 or TSC2 null cells, the level of phosphorylated Akt Serine473, a substrate of mTORC2, was decreased. This effect was also uncovered in tumor cells from TSC patients (Huang et al., 2008).

1.1.3.6 TBC1D7, the third partner of TSC1/TSC2 complex

TBC1D7 is identified as the third partner of TSC1/TSC2 complex which is found to associate with TSC1/TSC2 complex ubiquitously (Dibble et al., 2012). Disruption of TBC1D7 decreases the GTPase activating protein activity of TSC complex against Rheb and activates mTORC1 signaling. However, genetic sequencing studies did not find mutations in TBC1D7 locus of TSC patients.

1.1.4 Animal models of TSC

Various animal models have been created for detailed characterization of the cellular and molecular pathogenic process of TSC-associated tumors and for testing of potential therapeutic interventions.

1.1.4.1 The Eker rat

The Eker rat, with a spontaneous *Tsc2* mutation, was first discovered and maintained by Dr. Eker. Homozygous pups with *Tsc2* mutations died around embryonic day 11 (E11) and E12. *Tsc2* heterozygous rats developed renal cystadenomas, uterine leiomyomas, splenic hemangiosarcomas and brain subependymal lesions. The renal tumors in Eker rats showed the activation of mTORC1 pathway and had been used to test the efficacy of mTOR inhibitor in treating TSC1/2-null tumor cells.

1.1.4.2 *Tsc1*^{+/-} and *Tsc2*^{+/-} mice

Tsc1 and *Tsc2* knockout alleles were generated in 1999-2002 (Kobayashi et al., 1999; Kobayashi et al., 2001; Kwiatkowski et al., 2002; Onda et al., 1999). *Tsc1*^{-/-} and *Tsc2*^{-/-} embryos died at mid-gestation stage during development. *Tsc1*^{+/-} and *Tsc2*^{+/-} mice showed similar phenotypes characterized by development of cystadenomas in the kidney and hemangiomas in the liver. They were also found to have impaired spatial learning capacities. The tumor growth and neurocognitive defects in these model could be reversed by mTOR inhibition.

1.1.4.3 Tissue-specific Tsc1/2 knockout model, brain

An astrocyte specific Tsc1 knockout was generated by crossing a floxed allele of Tsc1 (Tsc1^{fl/fl}) and GFAP-Cre allele (Uhlmann et al., 2002). These mice showed increased number of astrocytes in the brain and developed seizures at around 2 month old with a median survival of 12 weeks.

Meikle et al, reported a neuronal specific Tsc1 knockout mouse model using synapsin I-Cre (Meikle et al., 2007). These mice developed seizures and displayed enlarged neurons in the cerebral cortex and hippocampus. They also displayed defects in neuronal myelination.

Another study targeted Tsc1 specifically in a portion of neuronal progenitor cells using doxycyclin inducible Nestin-Cre (Goto et al., 2011). These mice developed severe seizures and premature death which can be rescued by mTOR inhibitor treatments. Interestingly these mice showed vacuolated enlarged cells similar with giant cell observed in cortical tubers of TSC patients.

Two mouse models which develop human subependymal nodules (SEN) like lesions were generated using EMX1-Cre to target embryonic telencephalic neural stem cells and tamoxifen-inducible Nestin-Cre to target neuronal progenitor cells respectively (Magri et al., 2011; Zhou et al., 2011). These two studies reported for the first time that human TSC lesions in the lateral ventricle region were reproduced in mice and proved their neural stem cell origin.

Deletion of Tsc1 in Purkinje cells of mouse cerebellum using L7-cre led to autism-like behavior of the mutant mice (Tsai et al., 2012). mTOR inhibition by rapamycin reversed the behavioural defects.

1.1.4.4 Tissue-specific Tsc1/2 knockout model, kidney

Disrupting Tsc1 in a subset of epithelial tubular cells in kidney induced the formation of multiple cysts due to activation of mTORC1 since this phenomenon could be rescued by rapamycin treatment (Zhou et al., 2009).

1.1.4.5 Tissue-specific Tsc1/2 knockout model, heart

Targeting Tsc1 in cardiovascular tissue using smooth muscle protein-22 (SM22) Cre resulted in ventricular hypertrophy as a result of mTOR activation in Tsc1 null cells and a median survival of 24 days (Malhowski et al., 2011). Rapamycin treatment led to longer survival and decreased ventricular hypertrophy of the mutants.

1.1.4.6 Mouse models for mesenchymal tumors in kidney and lung

Mesenchymal tumors in the kidney and lung are major sources of morbidity and mortality of TSC adult patients. However, they have never been reproduced in currently available TSC animal models. Their cell of origin is unknown and the molecular nature underlying the proliferation and differentiation during their initiation and progression processes remain to be defined.

1.1.5 Treatment

The safety and efficacy of mTOR inhibitor (Everolimus) in treating TSC patients were tested first in a Phase I/II clinical trial on SEGA, later in two Phase III, randomized, double-blind and placebo-control clinical studies on SEGA, Angiomyolipoma and sporadic Lymphangiomyomatosis (Bissler et al., 2013; Franz, 2013). Everolimus has been shown to be effective in reducing the tumor size and approved for the treatment of TSC-associated SEGA and Angiomyolipomas. However, the tumors started regrowth when the treatment was discontinued. Furthermore, long term administration of mTOR inhibitors have undesirable side effects, including dyslipidemia, hyperglycaemia, stomatitis, skin rash, lung fibrosis, leucopenia and anaemia.

1.2 Hippo-YAP signaling

1.2.1 Hippo signaling network

Hippo signaling pathway is another critical regulator of organ size during development in addition to the Insulin pathway, first identified in *Drosophila* and conserved in mammals (Halder and Johnson, 2011; Pan, 2010; Tapon and Harvey, 2012; Yu and Guan, 2013). A kinase cascade is in the center of Hippo pathway which consist of the Ste20-like protein kinase Hippo (MST1/2 in mammals) and the NDR family protein kinase Warts (Lats1/2 in mammals), disruption of which lead to tissue overgrowth and tumorigenesis in *Drosophila* and mice. Warts (Lats1/2 in mammals) kinase in turn phosphorylates and inactivates transcriptional coactivator Yorkie (YAP/TAZ in mammals), the downstream effector of Hippo pathway.

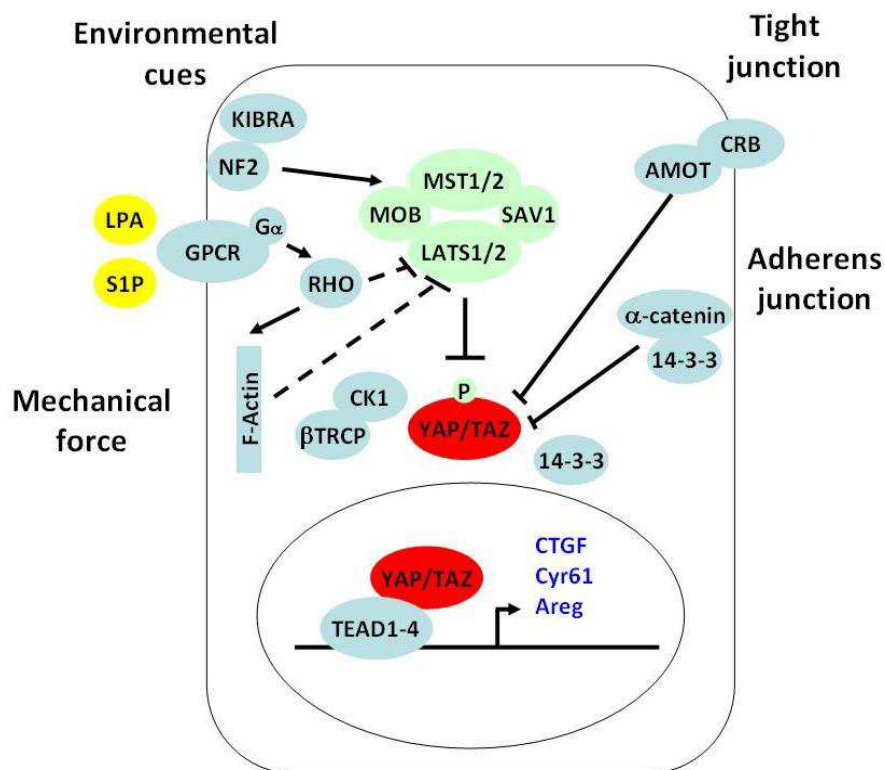


Figure 2. Hippo-YAP signaling pathway.

1.2.2 YAP/TAZ transcriptional coactivators

YAP and its homolog TAZ are the major downstream effectors of Hippo pathway which shuttle between cytoplasm and nucleus. In nucleus, they function as transcriptional coactivators interacting with specific transcription factors to regulate the transcription of downstream target genes. YAP has been shown to be a master regulator of tissue growth. YAP null embryos die at embryonic day 8.5 (Morin-Kensicki et al., 2006), while TAZ null mice appear viable (Hossain et al., 2007). YAP and TAZ double mutant embryos could not even survive the 16-cell morula stage during development. Overexpression of YAP in the mouse liver, intestine and skin lead to massive tissue overgrowth and tumorigenesis (Camargo et al., 2007; Dong et al., 2007; Schlegelmilch et al., 2011). YAP plays a critical role in promoting the anchorage-independent growth and epithelial to mesenchymal transition (EMT) of cancer cells in vitro (Zhao et al., 2007). Nuclear localization of YAP have been observed in about 60% human hepatocellular carcinomas, 15% human ovarian cancers and 65% human non-small-cell lung cancers (Wang et al., 2010; Xu et al., 2009; Zhang et al., 2011). Thus, YAP is identified to be an oncoprotein.

Several DNA-binding transcription factors have been shown to be associated with YAP, such as the Runt family member Runx2 (Yagi et al., 1999), the p53 family member p73 (Strano et al., 2001) and TEAD/TEF family transcription factors (Vassilev et al., 2001). TAZ has also been found to interact with a panel of transcription factors including Runx2, thyroid transcription factor 1, PPAR α , Tbx5, TEAD1, Pax3, and Smad2/3/4. Among these transcription factor, TEAD/TEF family transcription factors 1-4 (TEAD1-4, Sd in *Drosophila*) were demonstrated to be the critical mediators of the physiological functions of YAP/TAZ in Hippo pathway (Chan et al., 2009; Ota and Sasaki, 2008; Zhang et al., 2009; Zhao et al., 2008). Multiple transcriptional downstream target genes of YAP/TAZ have been identified, such as connective tissue growth factor (CTGF), the EGF family member amphiregulin (AREG), Cyr61 and IAP family member BIRC5.

1.2.3 Regulation of YAP/TAZ in mammals

1.2.3.1 Phosphorylation-dependent cytoplasmic sequestration

Phosphorylation of YAP on Serine127 by Lats1/2 kinase leads to its binding to 14-3-3 and cytoplasmic sequestration. This mechanism is conserved in TAZ and Yki. A number of upstream signals regulate YAP in this manner. Cell mechanical property changes such as disruption of stress fibres F-actin or actin contractility caused phosphorylation and nuclear export of YAP through RHO GTPase and Lats1/2 kinase (Dupont et al., 2011; Fernandez et al., 2011; Sansores-Garcia et al., 2011; Wada et al., 2011). Extracellular cues such as lysophosphatidic acid (LPA), sphingosine-1-phosphate (S1P) were also found to modulate YAP phosphorylation and cytoplasmic retention through G protein coupled receptors (GPCR)/RHO GTPase/Lats1/2 (Miller et al., 2012; Yu et al., 2012). In skin keratinocytes, YAP was phosphorylated by an unknown kinase and sequestered in the cytosol through binding to 14-3-3 and α -catenin (Schlegelmilch et al., 2011). Extra centrosomes in tetraploid cells led to YAP phosphorylation and inhibition through Lats1/2 activation by modulating small GTPase Rac1 and RhoA (Ganem et al., 2014). Additionally, a diversity of proteins modulate YAP phosphorylation and cytoplasmic retention through regulating its upstream kinases including Merlin, Kibra, RASSFs, PP2A, TAO, MARK1/PAR1 and SIKs.

1.2.3.2 Phosphorylation-dependent degradation through ubiquitin-proteasome pathway

Lats1/2 kinase could also phosphorylate YAP on Serine381 which primes the subsequent phosphorylation of YAP by CK1delta/epsilon leading to the recruitment of the E3 ubiquitin ligase SCF(β -TRCP). β -TRCP promotes the ubiquitination of YAP and its degradation by the proteasome (Zhao et al., 2010).

1.2.3.3 Phosphorylation-independent regulation

Angiotensin has been shown to directly bind to YAP and lead to its association with tight junctions (Zhao et al., 2011). In addition, multiple proteins directly interact with YAP/TAZ to modulate their activities in different contexts including WW domain-binding protein 2 (WBP2) (Chen et al., 1997), multiple ankyrin repeats single KH domain-containing protein (MASK) (Sidor et al., 2013), zona occludens protein 1 (ZO1), ZO2 (Oka et al., 2010), homeodomain-interacting protein kinase 2 (HIPK2) (Poon et al., 2012).

1.2.4 Crosstalk between two master regulators of organ size, mTOR signaling and Hippo-YAP signaling

Genetic studies have shown that the Tuberous Sclerosis Complex (TSC) 1/TSC2/mammalian Target Of Rapamycin (mTOR) and the Hippo/Yes-associated protein 1 (YAP) pathways are master regulators of organ size, which are often involved in tumorigenesis. The crosstalk between these signal transduction pathways in coordinating environmental cues, such as nutritional status and mechanical constraints, is crucial for tissue growth. YAP has been shown to regulate mTOR activity through modulating PTEN expression level by mir29 (Tumaneng et al., 2012b). EGF/PI3K/PDK1 regulates YAP dephosphorylation and nuclear localization in a Akt/mTOR independent mechanism (Fan et al., 2013; Strassburger et al., 2012). Whether and how mTOR regulate YAP remains elusive.

2 Results

2.1 Generation of mosaic-*Tsc1*KO mice which develop multisystem lesions showing similarities with human TSC.

Since TSC is a multiorgan mosaic disease with early manifestations in infancy and childhood, we generated mice that were homozygous for a floxed *Tsc1* allele (*Tsc1^{fl/fl}*), and carried a ubiquitously expressed and temporally regulated Cre transgenic allele (*CAGGCre-ERTM*) (Hayashi and McMahon, 2002; Meikle et al., 2007). Depending on the dose of Tamoxifen (TM), *Cre-ERTM* stochastically causes recombination of floxed alleles in a variable percent of cells in every tissue (Hayashi and McMahon, 2002), thus potentially targeting cells that give rise to the heterogeneous lesions. To circumvent the embryonic lethality of the whole body *Tsc1* deletion, we injected a relatively low dose of TM (10 mg/kg) intraperitoneally to pregnant dams at embryonic day 15.5 (E15.5). *Cre-ERTM*-positive pups were viable at birth and reached young adulthood at the same Mendelian frequency as the control littermates. However the majority of *Cre-ERTM*-positive mice did not survive over 10 weeks of age. We therefore focused our analysis on 6 week-old mice before the onset of lethality. At this age, recombination of the *Tsc1* allele was seen in every organ analysed at 30% - 80% frequency, depending on the organ (Fig. 3a). These data indicate that generalized mosaicism for complete *Tsc1* loss was achieved in these mice. Henceforth, these mutant mice are named mosaic-*Tsc1*KO.

Histological analysis of mosaic-*Tsc1*KO mice was performed in multiple tissues, with special attention to anatomical locations that are commonly affected in TSC. The cerebral cortex revealed a disorganization of the cortical layers and the presence of enlarged dysplastic neurons immunoreactive with antibodies against phosphorylated ribosomal protein S6 (rpS6), a marker of mTORC1 activity (Fig. 3b), as previously observed upon brain specific deletion of *Tsc1* (Meikle et al., 2007; Zhou et al., 2011). Furthermore, the dermal layer of the skin was thickened while the hypodermal fat layer was severely reduced, as assessed by Trichrome staining (Fig. 3c). The vessels decorated by ICAM-1 antibodies were increased in numbers and

abnormally enlarged in the dermal and muscular layers of the skin of mosaic-*Tsc1*KO mice. Macroscopically, the fur of the mutant mice was fairer than in their littermates (data not shown). Kidneys were enlarged and highly susceptible to haemorrhage (Fig. 4a). Kidney failure was underscored by a three fold increase of the plasma urea levels (Fig. 3d). In conclusion, the mosaic-*Tsc1*KO mice develop a multisystem and early-onset disease resembling different aspects of human TSC.

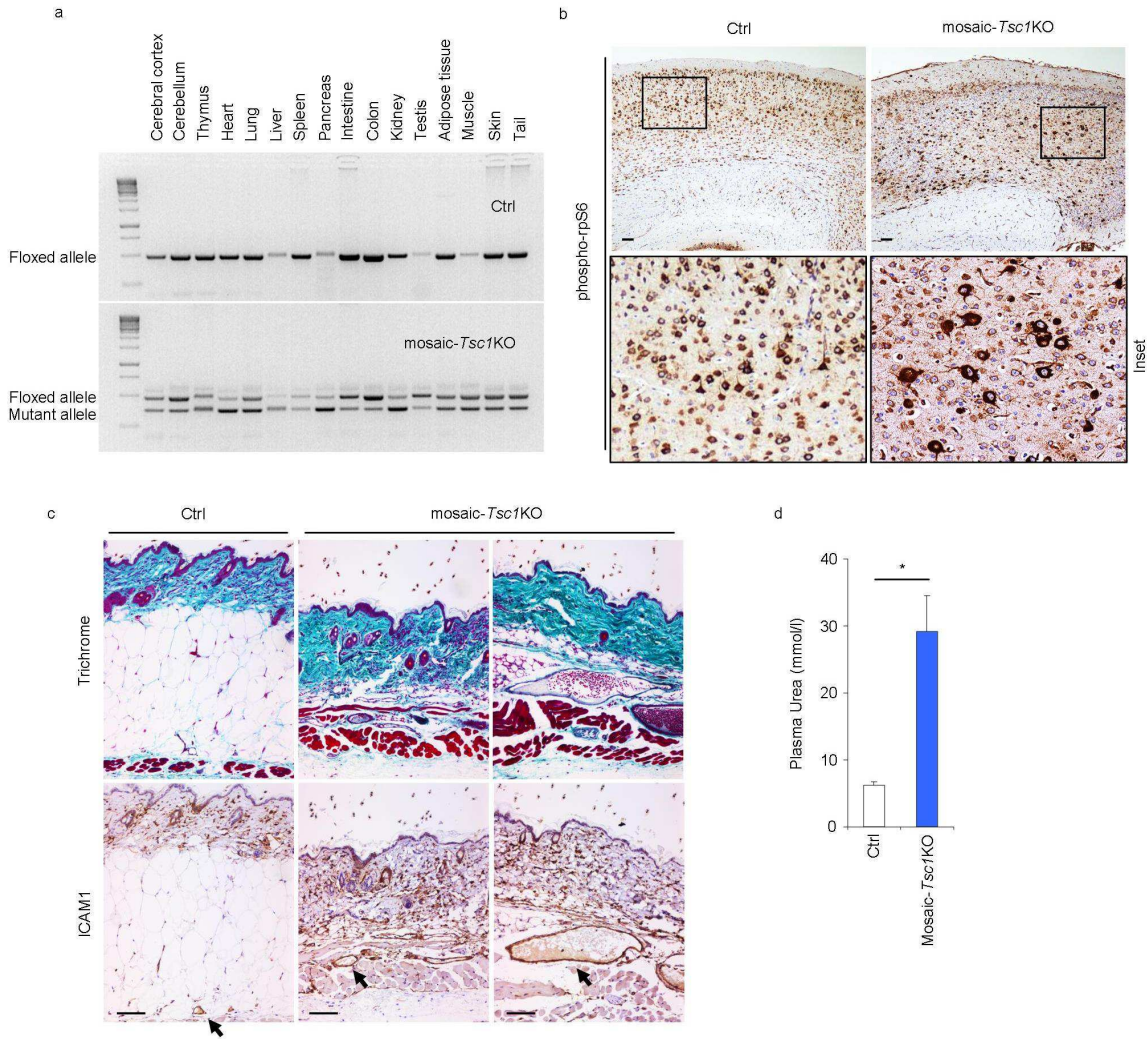


Figure 3. Mosaic-*Tsc1*KO mice develop multisystem lesions showing similarities with human TSC. (a) Genomic DNA was prepared from control (ctrl) and mosaic-*Tsc1*KO mice 1.5 months after tamoxifen injection, and the floxed/mutant alleles were detected by PCR in the indicated organs. (b) Expression of phospho-rpS6 in cerebral cortex sections from ctrl and mosaic-*Tsc1*KO mice was analyzed by immunohistochemical staining. (c) Skin samples of ctrl and mosaic-*Tsc1*KO mice were stained for ICAM-1 expression and using Trichrome. Arrows indicate ICAM-1 positive vessels. (d) Plasma urea concentrations were determined in ctrl and mosaic-*Tsc1*KO kidneys (Mean \pm s.e.m., N=4 mice/group, * p <0.05). Scale bar, 100 μ m. Three independent pregnant females were injected with Tamoxifen. For immunohistochemistry analysis, similar stainings were found in four different ctrl/mosaic-*Tsc1*KO mice (6 weeks of age, two sections per each mouse).

2.2 Mosaic-*Tsc1*KO mice develop renal mesenchymal lesions recapitulating PEComas associated with human TSC.

We investigated whether the stochastic *Tsc1* deletion at E15.5 of embryogenesis targets cells giving rise to mesenchymal lesions, such as PEComas. We examined the mutant kidneys in detail, as the observed haemorrhages might be due to vascular lesions, and haemorrhage is an important complication of TSC renal angiomyolipoma (Bissler et al., 2013). Consistent with the phenotype in other TSC mutant animal models (Onda et al., 1999; Zhou et al., 2009), the mosaic-*Tsc1*KO kidneys were polycystic, a sign of abnormal proliferation of tubular epithelial cells (Fig. 4b). However, immunostaining with Vimentin antibody, a marker of mesenchymal cells, revealed several lesions (Fig. 4b), appearing as small, well defined, fasciculated nodules (Fig. 4c). Cells within the lesions expressed additional mesenchymal markers, such as H-Caldesmon and α -smooth muscle actin (α SMA) (Fig. 5a and 5b). These nodules were proliferative, as demonstrated by immunostaining with Ki67 antibodies, and displayed high mTORC1 signalling, as shown by phosphorylation of rpS6 (Fig. 4c). They were frequently observed near vessels (Fig. 4c), and/or contained disorganized vascular components highlighted by CD31-positive endothelial cells and PDGF receptor β -, α SMA- double positive pericytes (Fig. 5a and 5b). Importantly, these mesenchymal lesions also showed immunoreactivity with the HMB45 antibody recognizing the melanocytic marker Pmel (also named gp100), which is a pathognomonic feature of PEComas (Fig. 4d). Moreover the mRNA levels of several melanocytic markers including Mart1, Cathepsin K, Pmel, Tyrp1 were sharply increased in mutant kidneys (Fig. 4e). Finally, immunoblot analysis of protein extracts confirmed the induction of both melanocytic (Mart1) and myogenic markers (α SMA), along with mTORC1 activation in mosaic-*Tsc1*KO kidneys (Fig. 4f). To monitor Cre recombinase activity within the lesions, the mosaic-*Tsc1*KO mice were crossed with transgenic mice carrying a flox-stop-flox-lacZ reporter at the Rosa26 locus. As shown in Fig. 5c, the epithelial cells lining the cysts and the majority of the cells in the mesenchymal lesions underwent Cre-mediated recombination and were therefore *Tsc1* deficient.

To directly compare the mesenchymal lesions found in mosaic-*Tsc1*KO kidneys with human specimens, we screened samples of renal angiomyolipomas occurring in TSC patients. As shown in Fig. 4g, the majority of human angiomyolipomas were surrounded by a number of smaller lesions, so called microhamartomas (or microscopic angiomyolipomas), which shared the common expression of cathepsin K, α SMA and Pmel. It is likely that the small lesions represent early developmental stage of angiomyolipomas. Importantly, these microhamartomas exhibited a striking similarity with their murine counterparts in terms of morphology and immunophenotype. In conclusion, mosaic-*Tsc1*KO mouse kidneys develop renal mesenchymal lesions similar with PEComas observed in human TSC patients. However we did not observe any kidney angiomyolipomas in these mice. This may be due to the premature mortality seen in these mice, precluding further lesion development into full blown angiomyolipomas.

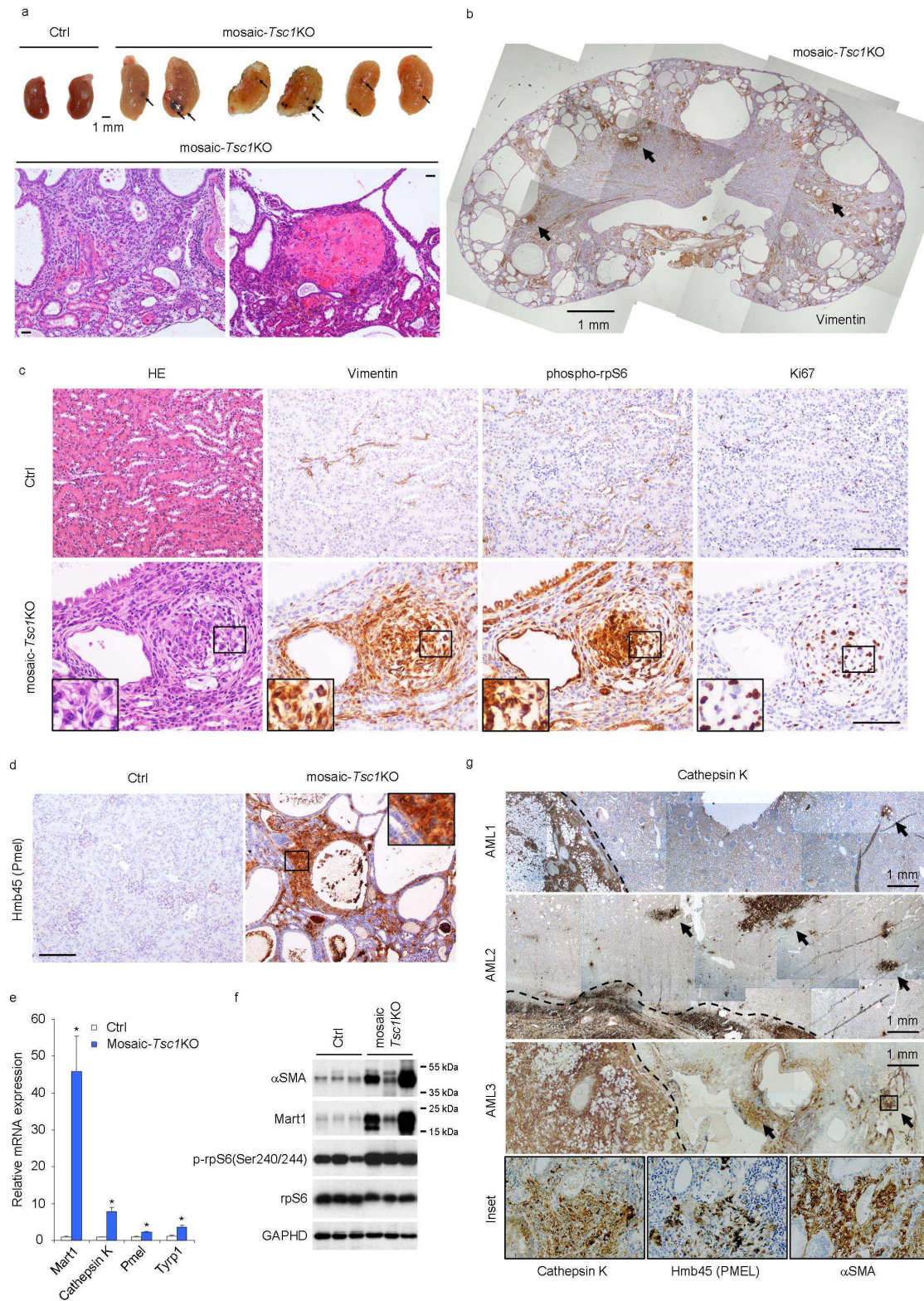


Figure 4. Mosaic-*Tsc1*KO mice develop renal mesenchymal lesions recapitulating PEComas associated with human TSC. Kidneys from ctrl (N=3) and mosaic-*Tsc1*KO (N=3) mice were analyzed at 6 weeks of age. (a) Macroscopic photos and representative H&E staining. Arrows indicate hemorrhages. (b-d) Expression of vimentin (b, c), phospho-rpS6 and Ki67 (c) and Hmb45/Pmel (d) was assessed by immunohistochemistry. H&E staining was shown on left in panel c. Arrows in panel b indicate vimentin-positive micro-hamartomas in mosaic-*Tsc1*KO kidneys. For immunohistochemistry analysis, similar stainings were found in three different ctrl/mosaic-*Tsc1*KO mice (three sections per each mouse). (e) Expression of Mart1, Cathepsin K, Pmel and Tyrp1 mRNA was assessed by qRT-

PCR. (Mean \pm s.e.m., N=3 mice/group, *p<0.05). (f) Expression of α SMA, Mart1, p-rpS6, and total rpS6 protein was assessed by immunoblot. (g) Expression of the indicated proteins in three distinct human angiomyolipoma (AML) samples was assessed by immunohistochemistry. Arrows indicate the micro-hamartoma. Scale bar, 100 μ m unless otherwise indicated. Insets show higher magnification of the lesions indicated with squares.

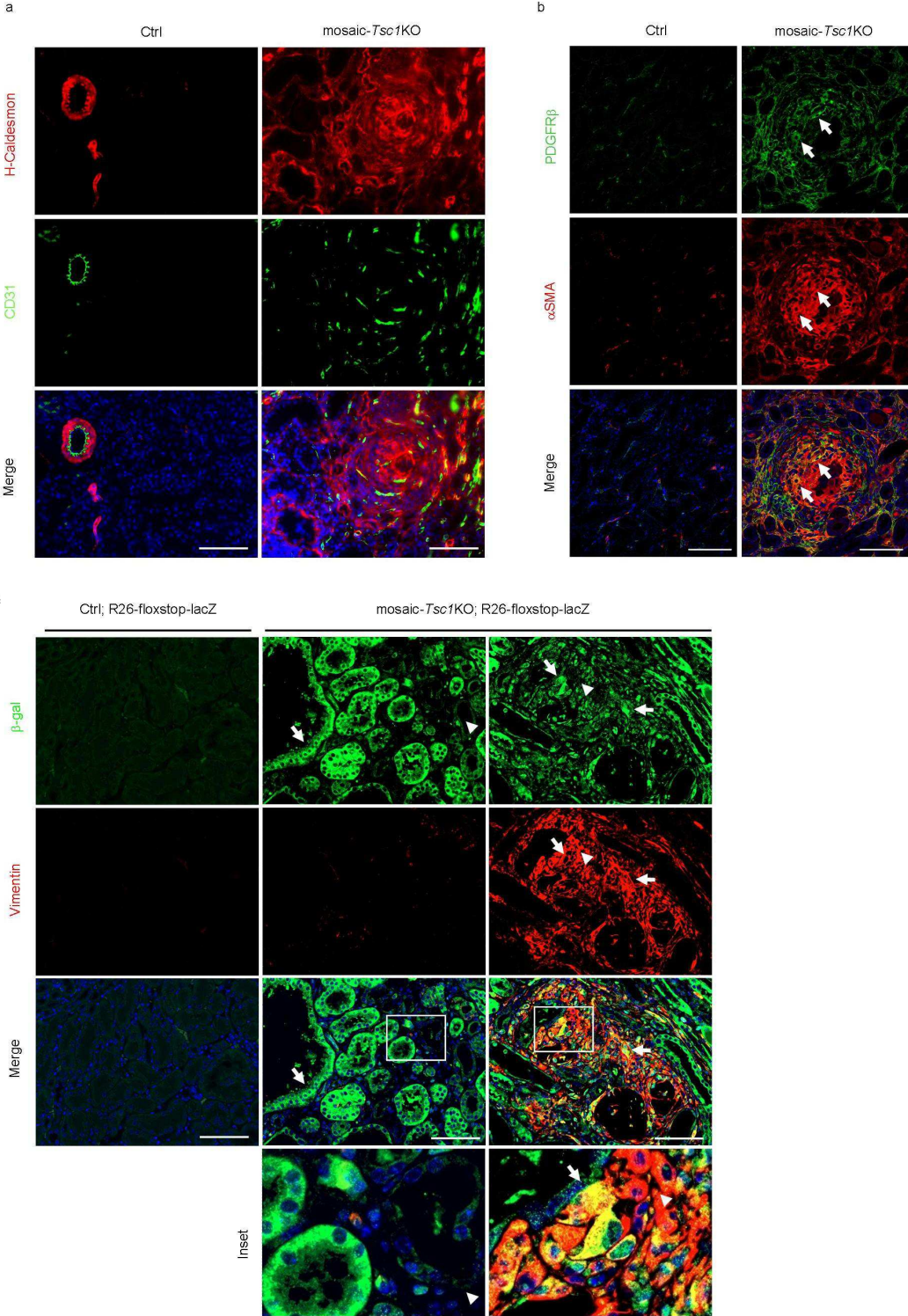


Figure 5. Mosaic-*Tsc1*KO mice develop renal H-caldesmon⁺ mesenchymal lesions containing CD31⁺ endothelial cells and PDGFR β ⁺/ α SMA⁺ pericytes. (a, b) Kidney tissues were isolated from

ctrl and mosaic-*Tsc1*KO mice at 6 weeks of age and analyzed by immunofluorescence for H-caldesmon and CD31 (a) or PDGFR β and α SMA (b). Arrows in (b) indicate PDGFR β and α SMA double positive pericytes. Scale bar, 100 μ m. (c) Expression of β -gal and vimentin on kidney sections from Ctrl;R26-floxstop-LacZ and mosaic-*Tsc1*KO;R26-floxstop-LacZ mice was assessed by immunofluorescence. Arrows indicate β -gal positive cells and arrowheads show β -gal negative cells. Insets show higher magnification of tissue indicated with squares. Scale bar, 100 μ m. Similar stainings were found in three different mice/genotype (three sections per each mouse).

2.3 YAP is up-regulated by mTOR in renal lesions of mosaic-*Tsc1*KO mice and human angiomyolipoma.

The phenotype of mosaic-*Tsc1*KO mouse kidneys consisted of enlarged organ size, polycystosis and microscopic PEComas. To gain mechanistic insights, we screened transcriptional outputs of developmental pathways involved in tissue growth, planar cell polarity, and multipotency. These included target genes of Notch, Wnt, Hedgehog and Hippo pathways (data not shown and Fig. 6a). Of note, the mosaic-*Tsc1*KO kidneys had a two to eight fold increase in mRNA levels of connective tissue growth factor (CTGF), amphiregulin (Areg), and Cyr61, all known transcriptional targets of the Hippo pathway (Tumaneng et al., 2012a). This stimulation was blunted by treating the mice every other day for two weeks with the rapamycin derivative Temsirolimus (5 mg/kg), suggesting a tight control of the Hippo pathway by mTOR in *Tsc1* mutant kidneys. Next, we examined the levels of YAP, whose function is required for the transcriptional regulation of CTGF, Areg and Cyr61 downstream of the Hippo pathway. While YAP mRNA levels were not affected by *Tsc1* deletion and mTOR inhibition (Fig. 6a), the protein amount tightly correlated with mTORC1 activity as assessed by phosphorylated rpS6 levels in kidneys (Fig. 6b). The increase in YAP levels was detected both in cytosol and nuclei (Figure 6c). TAZ, the homolog of YAP, was also up-regulated at the protein level in mosaic-*Tsc1*KO kidneys (Fig. 6b).

To localize the kidney cell compartment expressing YAP, immunostaining was performed (Fig. 6d). In adult floxed control littermates, YAP was found in scattered tubular epithelial cells of the kidney cortex. Strikingly, *Tsc1* deletion caused a widespread expression of YAP in both tubular epithelial cells lining the cysts and in spindle shaped mesenchymal cells of the kidney cortex. Notably, in the mosaic-

*Tsc1*KO mouse kidneys a large fraction of YAP was localized in the nuclei, consistent with an active function as a transcriptional regulator.

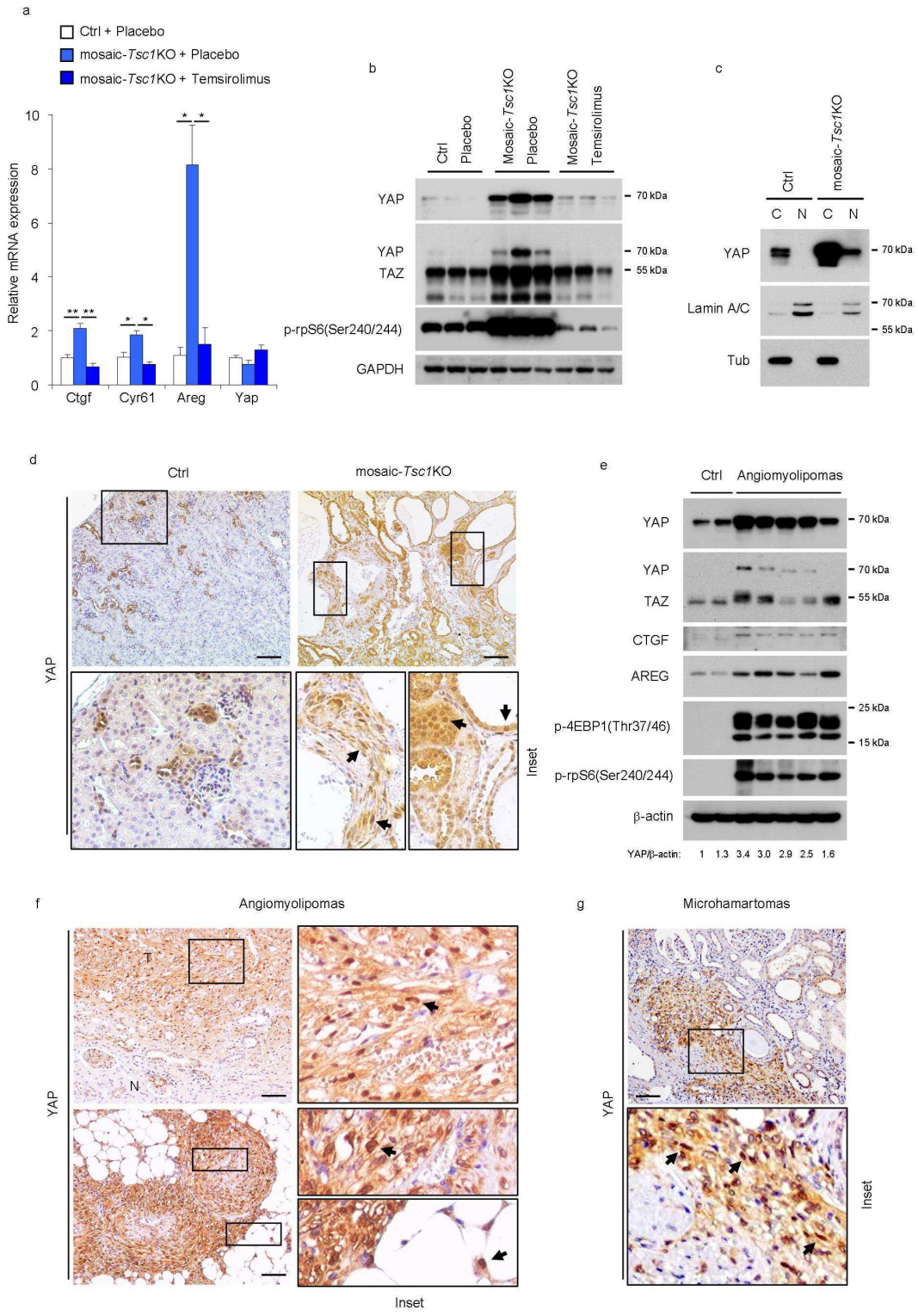


Figure 6. YAP is up-regulated by mTOR in renal lesions of mosaic-*Tsc1*KO mice and human angiomyolipoma. (a, b) Expression of indicated genes was determined by qRT-PCR (a) and immunoblot analysis (b) in kidney samples from Ctrl mice treated with placebo, mosaic-*Tsc1*KO mice treated with placebo or temsirolimus. Mice were injected intraperitoneally with vehicle or temsirolimus

(5 mg/kg) every other day for two weeks before sacrifice. Mice were sacrificed at 6 weeks of age. (Mean \pm s.e.m., N=3 mice/group, * p <0.05, ** p <0.01). (c) Expression of indicated proteins was analysed by immunoblot in nuclear and cytoplasmic protein extractions from ctrl and mosaic-*Tsc1*KO mouse kidney samples. Similar results were found in three different mice/genotype. (d) YAP expression was assessed on kidney sections from ctrl and mosaic-*Tsc1*KO mice by Immunohistochemistry. Arrows indicate cells with YAP nuclear localization. Scale bar, 100 μ m. Similar stainings were found in three different mice/genotype (three sections per each mouse). (e) Expression of indicated proteins was analysed by immunoblot in control human kidney and angiomyolipoma samples. (f, g) YAP expression was analysed by immunohistochemistry on human angiomyolipoma samples (N, normal kidney; T, Tumor). Arrows indicate cells with YAP nuclear localization. Scale bar, 100 μ m. Insets show higher magnification of the lesions indicated with squares. Similar results were found in 7/7 different human angiomyolipoma samples.

To determine whether the activation of the YAP pathway also occurred in human TSC, first we examined YAP, CTGF, and Areg protein levels in TSC angiomyolipomas by immunoblotting (Fig. 6e). The activation of mTORC1, as assessed by 4EBP1 and rpS6 phosphorylation, and the increased YAP protein were seen in all samples examined. Importantly, the transcriptional targets CTGF and Areg were also expressed at higher levels in angiomyolipomas. Since the levels of TAZ were more variable among the human samples analysed, we decided to focus our analysis on YAP in this study. Next, we analyzed YAP localization in the different cell types of human angiomyolipomas and in the adjacent kidney structures. As shown in Fig. 6f, high levels of YAP immunoreactivity were detected in all cell types that could be found in angiomyolipomas, i.e. adipocytes, smooth muscle cells and blood vessel components. In the adjacent kidney regions, YAP protein was almost undetectable, except for small YAP-positive cysts of epithelial origin lining the lesion. The YAP antibody also stained small human renal renal micro-hamartomas that closely resembled the mesenchymal lesions observed in mosaic-*Tsc1*KO mouse kidneys (Fig. 6g). Finally, we examined other human TSC-related PEComas from different organs. In pulmonary lymphangioliomyomatosis, hepatic angiomyolipomas, as in renal angiomyolipomas, YAP expression invariably correlated with mTORC1 activity in tumor cells (Fig. 7). After screening a total of ten PEComas, YAP was found to be consistently highly expressed in all the specimens, and may be considered as a novel marker. Interestingly, we detect YAP expression already at early stages of human PEComa development, suggesting a putative role in the origin of the lesion. In addition, YAP upregulation and nuclear localization was also observed in TSC-associated brain tumor SEGA (Fig. 8).

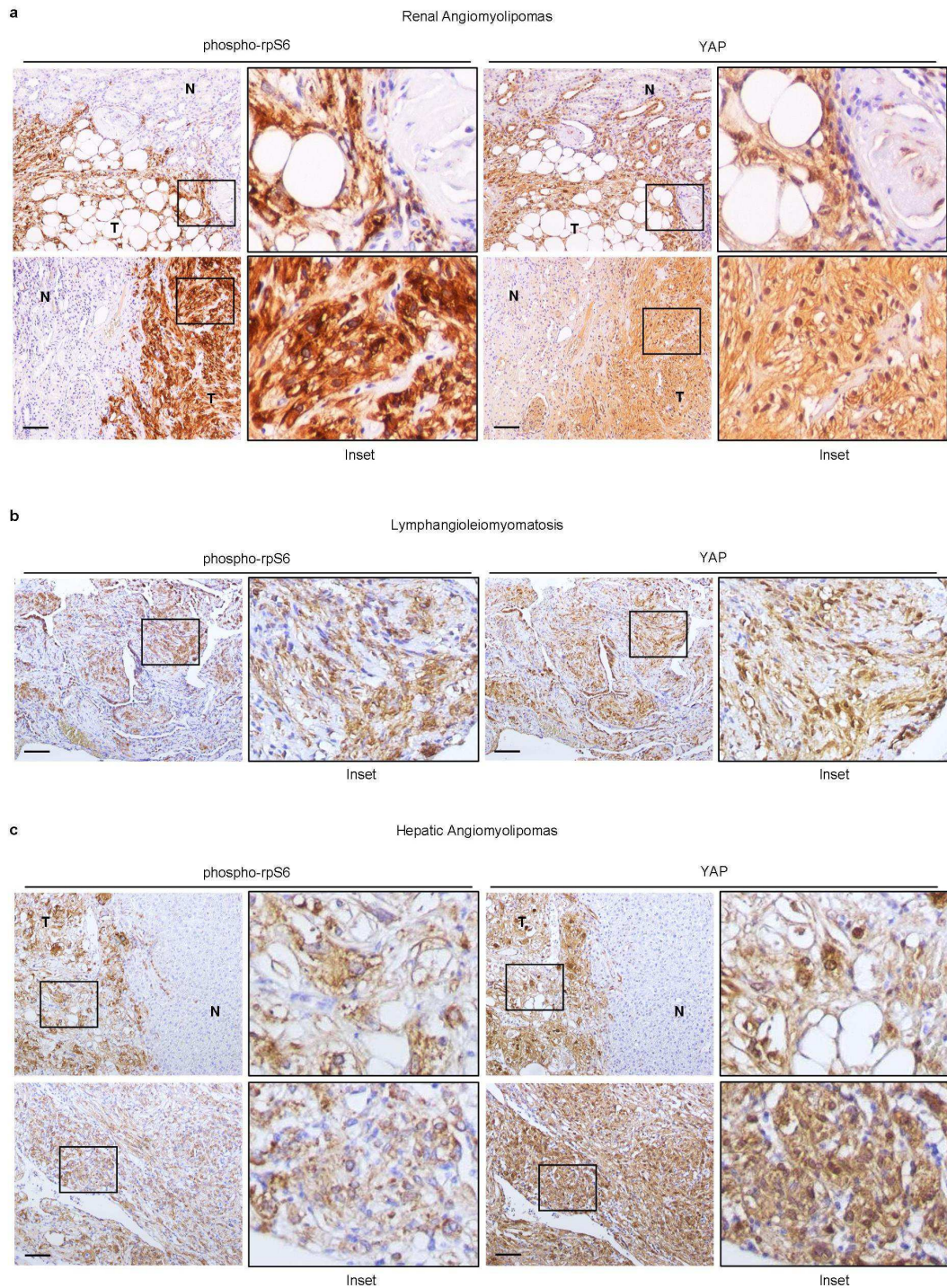


Figure 7. YAP levels correlates with rpS6 phosphorylation in human TSC-related PEComas.

(a, b, c) Immunohistochemical analysis of rpS6 phosphorylation and YAP expression in human PEComa samples associated with TSC (a, renal angiomyolipomas; b, pulmonary lymphangioliomyomatosis; c, hepatic angiomyolipoma) (N, normal tissue; T, Tumor). Scale bar, 100 μ m.

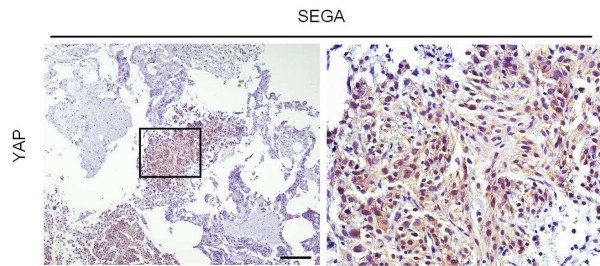


Figure 8. YAP upregulation and nuclear localizaiton in human TSC-related SEGA. Immunohistochemical analysis of YAP expression in human SEGA samples associated with TSC. Scale bar, 100 μ m.

2.4 YAP is required for the abnormal proliferation and survival of TSC1/2 null cells *in vitro*.

We then examined whether YAP contributed to the growth phenotype of TSC1/TSC2 deficient cells. We cultured mouse embryonic fibroblasts (MEFs) that were *Tsc2*^{-/-} and *Tsc2*^{+/+} MEFs, which were in *p53*^{-/-} background (Zhang et al., 2003). YAP protein levels were increased by three fold in the *Tsc2* null cells (Fig. 9a). This effect was also observed in nuclear fractions (data not shown), and was paralleled by increased expression of the YAP target CTGF (Fig. 9a and 9g). Thus the up-regulation of the YAP pathway can also be observed in a cell autonomous manner upon TSC complex deficiency. This effect could not be ascribed to a relief of Hippo/Lats inhibition of YAP in *Tsc2* null cells, because the amount of Ser112-phosphorylated YAP, a site of the Lats1/2 kinases (Zhao et al., 2010), paralleled the increase in total YAP protein in the mutant cells (Fig. 9a). *Tsc2* deletion is known to provide a proliferative advantage over wild type controls in serum starvation conditions (Zhang et al., 2003). After 24h of serum starvation, the phosphorylation of the mTORC1 substrate rpS6 and the YAP protein levels were shut off in controls while remaining high in *Tsc2*^{-/-} cells (Fig. 9b). As expected, cell counting over a three day-period after serum starvation indicated that the number of *Tsc2*^{-/-} cells steadily increased as opposed to wild type control (Fig. 9c). Importantly the proliferation of *Tsc2*^{-/-} cells was blunted by YAP knockdown (Fig. 9c and 9d). Cell viability was also sensitive to YAP levels, as indicated by the drop in cell number at the 72 hour time point (Fig. 9c), and the increase in TUNEL positive apoptotic cells (Fig. 9e). The

effect of YAP knockdown was mimicked by treatment with verteporfin, a compound that was reported to interfere with YAP binding to the TEAD1-4 transcription factors, and accordingly inhibited CTGF mRNA expression in *Tsc2*^{-/-} cells (Fig. 9f and 9g) (Liu-Chittenden et al., 2012). YAP levels were also increased after TSC1 and TSC2 knockdown by RNAi in human embryonic kidney 293 (HEK293) cells (Fig. 9h). The concomitant knockdown of YAP impaired the proliferative advantage of TSC1-depleted HEK293 cells in serum starved conditions (Fig. 9i). Taken together, these data demonstrate that YAP activity is, at least partly, required to promote proliferation of TSC complex deficient cells *in vitro*.

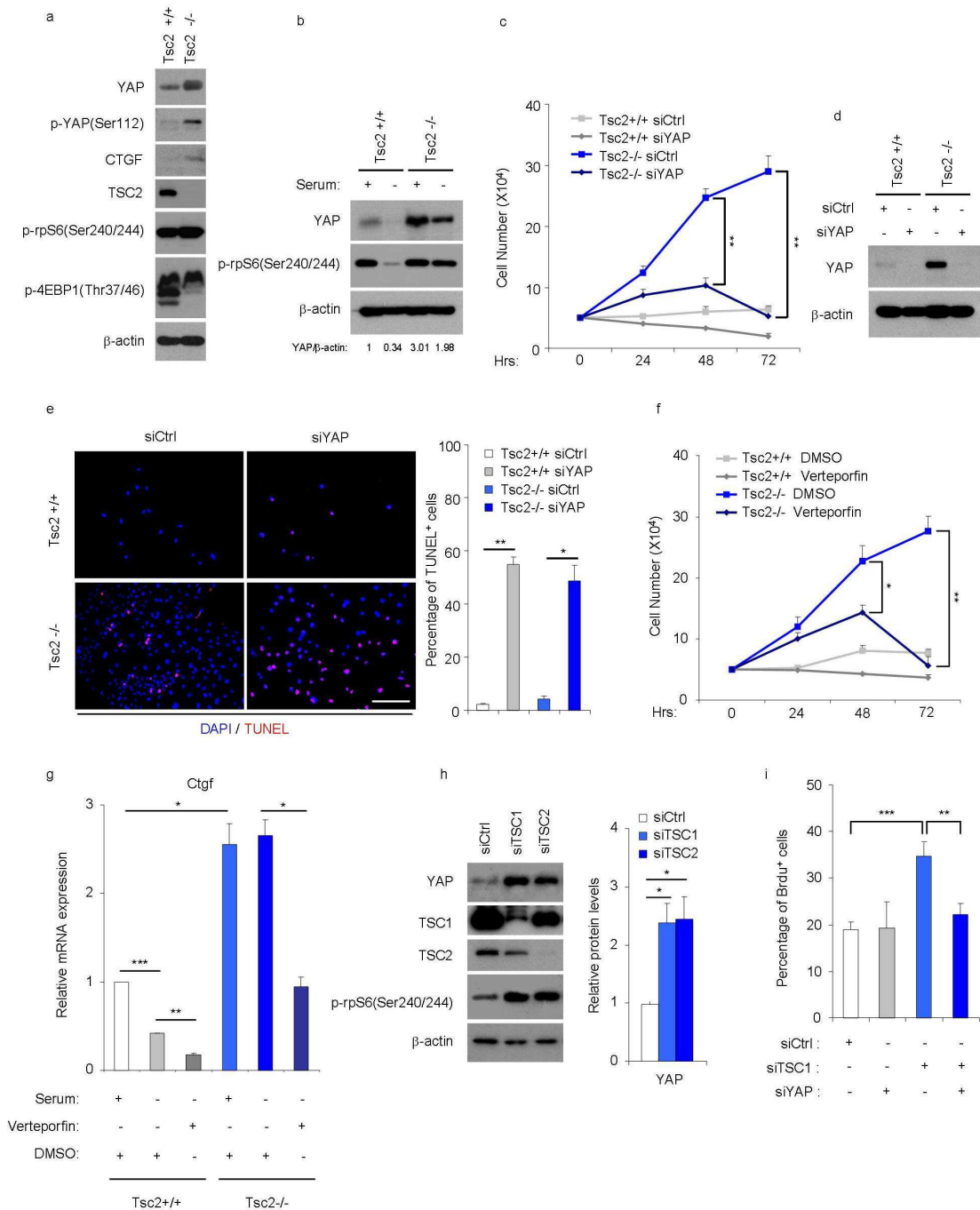


Figure 9. YAP is required for the abnormal proliferation and survival of TSC1/2 null cells *in vitro*.

(a, b) Expression of indicated proteins was analysed by immunoblot in *Tsc2*^{+/+} and *Tsc2*^{-/-} MEFs (these MEFs were generated in *p53*^{-/-} background) cultured with or without serum for 24 hours. Similar results were observed in three independent experiments. (c-e) *Tsc2*^{+/+} and *Tsc2*^{-/-} MEFs transfected with siCtrl or siYAP were cultured in serum starvation conditions for a 72-hour period. (c) Cell number was counted in different groups. Three independent experiments were performed and analysed (Mean \pm s.e.m., ***p*<0.01). (d) Expression of YAP protein was analysed by immunoblot at 24-hour time point. Similar results were observed in three independent experiments. (e) Apoptotic cells were identified by TUNEL assay at 48-hour time point. The percentage of TUNEL positive cells was determined by counting TUNEL-positive nuclei among at least 500 cells in distinct fields of each experiment. Three independent experiments were performed and analysed (Mean \pm s.e.m., **p*<0.05, ***p*<0.01). (f, g) *Tsc2*^{+/+} and *Tsc2*^{-/-} MEFs were cultured under serum starvation conditions and treated with DMSO or Verteporfin for a 72-hour period. (f) Cell number was counted. Three independent experiments were

performed and analysed (Mean \pm s.e.m., * p <0.05, ** p <0.01). (g) Expression of Ctgf mRNA was assessed by qRT-PCR in different treatments. Three independent experiments were performed and analysed (Mean \pm s.e.m., * p <0.05, ** p <0.01, *** p <0.001). (h) Expression of indicated proteins was analysed by immunoblot in HEK293 cells transfected with siRNAs against TSC1, TSC2 or siCtrl. YAP protein level was normalized with β -actin. Four independent experiments were performed and analysed (Mean \pm s.e.m., * p <0.05). (i) Percentage of BrdU positive HEK293 cells with indicated treatments under serum deprivation conditions for 24 hours was assessed by three-hour BrdU pulse-labeling before harvest. Three independent experiments were performed and analysed (Mean \pm s.e.m., ** p <0.01, *** p <0.001).

2.5 Inhibition of YAP pharmacologically or genetically attenuates abnormal proliferation and induces apoptosis of *Tsc1* null cells *in vivo*.

To assess the effects of YAP inhibition *in vivo*, mosaic-*Tsc1*KO and control mice were treated intraperitoneally with verteporfin (100 mg/kg) every other day for ten days (Liu-Chittenden et al., 2012). The YAP inhibitor reduced the kidney to body weight ratio by 50% (Fig. 10a), and attenuated overall kidney size and polycystosis in mutant mice without affecting control kidneys (Fig. 10b). These effects were concomitant to a reduction in CTGF expression (Fig. 10c). The proliferation of the mesenchymal lesions was severely affected by verteporfin treatment, as indicated by Ki67 staining of α -SMA positive cells (Fig. 10d). Furthermore, verteporfin treatment led to apoptosis of both epithelial and mesenchymal cells in mosaic-*Tsc1*KO kidneys (Fig. 10e). To specifically affect YAP expression by genetic means, we crossed *CAGGCre-ERTM*; *Tsc1^{fl/fl}* with *Tsc1^{fl/fl}*; *Yap^{fl/+}* mice. The offspring mice were injected with TM at postnatal day 2 (P2), in order to generate mosaic-*Tsc1*KO carrying a mutant allele of *Yap* (mosaic-*Tsc1*KO; *Yap^{+/-}*). The heterozygous deletion of *Yap* was sufficient to reduce YAP protein levels in mosaic-*Tsc1*KO mice (Fig. 11c). This was accompanied by a sharp attenuation of the kidney phenotype as compared to mosaic-*Tsc1*KO mice, as assessed by the kidney to body weight ratio (Fig. 11a), kidney size and polycystosis (Fig. 11b), and mesenchymal cell proliferation (Fig. 10d and 11e). The residual lesions observed in mosaic-*Tsc1*KO; *Yap^{+/-}* kidneys displayed rpS6 phosphorylation, suggesting efficient recombination (data not shown). Whole body heterozygous deletion of *Yap* (*Yap^{+/-}*) did not inhibit kidney growth and proliferation (Fig. 11f, 11g and 11h), indicating that the reduction of YAP gene

dosage was particularly effective in a background of *Tsc1* loss of function. Thus strategies targeting YAP activity might be beneficial in treating TSC related kidney overgrowth and PEComa formation.

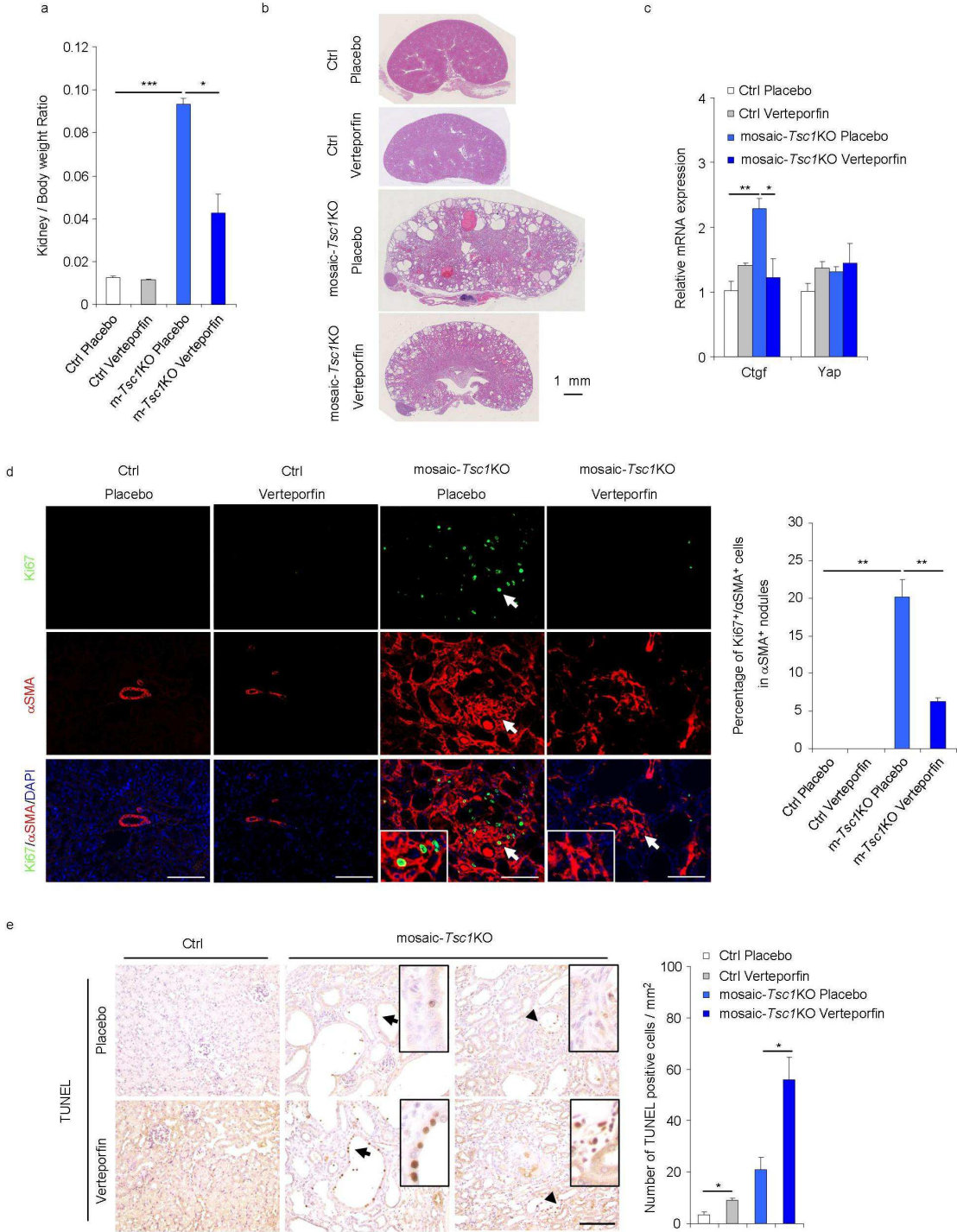


Figure 10. Verteporfin treatment inhibits proliferation and induces apoptosis of *Tsc1* null cells *in vivo*. Mice were administered intraperitoneally with vehicle or verteporfin at a dose of 100 mg/kg every other day for ten days before sacrifice. Mice were sacrificed at 6 weeks of age. Three

independent experiments were performed and mice in different treatments were pooled for analysis. (a) Kidney / Body weight ratio of Ctrl and mosaic-*Tsc1*KO mice treated with placebo or Verteporfin (N=3 mice/group, Mean \pm s.e.m, * $p < 0.05$, *** $p < 0.001$). (b) Representative pictures of Hematoxylin and eosin staining of kidney sections from Ctrl and mosaic-*Tsc1*KO mice treated with placebo or Verteporfin. Scale bar, 1 mm. (c) Expression of indicated mRNAs was analysed by qRT-PCR in kidney samples from Ctrl and mosaic-*Tsc1*KO mice treated with placebo or Verteporfin (N=3 mice/group, Mean \pm s.e.m, * $p < 0.05$, ** $p < 0.01$). (d) Percentage of Ki67 and α SMA double positive cells in α SMA positive mesenchymal lesions in the indicated kidneys. Immunofluorescence staining and counting were performed on three sagittal sections from different kidney regions for each mouse. Representative images are shown (Mean \pm s.e.m., N=3 mice/group, ** $p < 0.01$, Scale bar 100 μ m). Insets show the lesions indicated with arrows. (e) In situ apoptotic cells was assessed by TUNEL assay on the kidney sections from Ctrl and mosaic-*Tsc1*KO mice treated with placebo or verteporfin. The number of TUNEL positive cells were counted in ten distinct fields of each section. Three sections were analysed per each mouse. Representative images are shown. Arrows indicate TUNEL positive epithelial cells and arrowheads show TUNEL positive mesenchymal cells. Insets show the lesions indicated with arrows. Mean \pm s.e.m., N=3 mice/group, * $p < 0.05$, Scale bar 100 μ m.

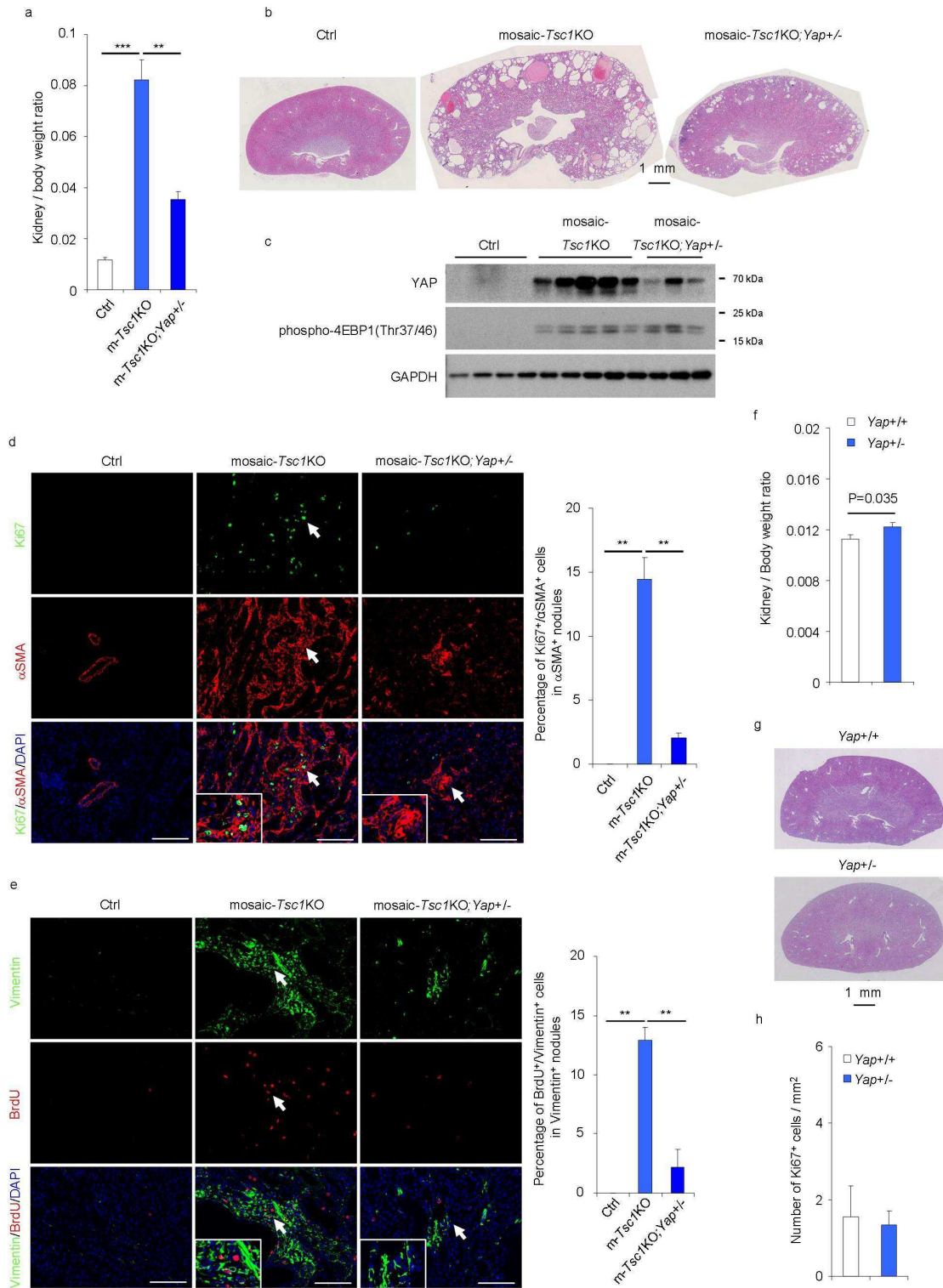


Figure 11. Heterozygous deletion of Yap compromises the proliferation of renal mesenchymal lesions in mosaic-Tsc1KO mice. Three independent tamoxifen injection experiments were performed and female mice of indicated genotypes were pooled for analysis. (a) Kidney/Body weight ratio of the indicated mice sacrificed at 6 weeks of age (Ctrl N=4, mosaic-Tsc1KO N=5, mosaic-Tsc1KO;Yap^{+/-} N=3). (b) Representative pictures of hematoxylin and eosin staining of kidney sections from the indicated mice. (c) Expression of indicated proteins was analysed by immunoblot in mouse kidney samples from the indicated genotypes. (d) Percentage of Ki67 and αSMA double positive cells in αSMA positive kidney lesions from mice of the indicated genotypes. Immunofluorescence staining and counting were performed on three sagittal sections from different kidney regions for each mouse

(Ctrl N=4, mosaic-*Tsc1*KO N=5, mosaic-*Tsc1*KO;*Yap*^{+/-} N=3). Insets show the lesions indicated with arrows. Scale bars, 100 μ m. Mean \pm s.e.m., ***p*<0.01. (e) Percentage of BrdU and Vimentin double positive cells in Vimentin positive mesenchymal lesions in the indicated kidneys. BrdU (50 mg/kg) was injected intraperitoneally 24 hours before sacrifice. Immunofluorescence staining and counting were performed on three sagittal sections from different kidney regions for each mouse. Representative images are shown (Ctrl N=4, mosaic-*Tsc1*KO N=5, mosaic-*Tsc1*KO;*Yap*^{+/-} N=3, mean \pm s.e.m., ***p*<0.01, Scale bar 100 μ m). Insets show the lesions indicated with arrows. (f) Kidney / Body weight ratio of *Yap*^{+/+} (N=3) and *Yap*^{+/-} (N=3) mice. (g) Hematoxylin and eosin staining of kidney sections from *Yap*^{+/+} and *Yap*^{+/-} mice. Scale bar, 1 mm. (h) Percentage of Ki67 positive cells per mm² in kidney sections from *Yap*^{+/+} and *Yap*^{+/-} mice (N=3). The number of Ki67 positive cells were counted in ten distinct fields per each section. Two sections were analysed per each mouse.

2.6 YAP is accumulated in TSC deficient cells due to blockage of autophagy in a mTOR-dependent manner.

YAP is under tight control by a variety of upstream regulators (Tumaneng et al., 2012a). To gain mechanistic insights into the novel crosstalk between the TSC1/TSC2/mTORC1 and YAP, we asked which step of YAP expression was affected in *Tsc2*^{-/-} cells. Consistent with the data in mosaic-*Tsc1*KO kidneys (Fig. 6a), the comparable YAP mRNA amount in *Tsc2*^{-/-} and *Tsc2*^{+/+} cells ruled out transcriptional effects (data not shown). We did not find evidence for a regulation at the step of translational initiation, as the recruitment of YAP mRNA in the polysomal fraction was also equivalent in the two genotypes (data not shown). A major node in YAP regulation is the phosphorylation on five serine residues by the Lats1/2 kinases that causes cytosolic retention and promotes protein degradation by the proteasome (Huang et al., 2005; Zhao et al., 2010). However no major alteration in Lats1/2 kinase activity was detected in *Tsc2*^{-/-} cells and kidney tissues, as indicated by the Ser-112 YAP phosphorylation (Fig. 6a and data not shown). Accordingly, 8 hour-treatment with the proteasome inhibitor MG132, while leading to a significant accumulation of polyubiquitinated proteins, did not affect YAP levels in either *Tsc2*^{-/-} or control cells in growing conditions (data not shown). Intriguingly, the YAP phosphorylation by Lats1/2 kinases has been reported to induce a rapid degradation of YAP in high density, but not in low density culture conditions (Zhao et al., 2010), the latter pertaining to the experimental setup used in this study. Thus, in growing cells with no contact inhibition and with high mTOR activity, YAP levels are controlled by an alternative mechanism.

TSC1/2 mutant cells have impaired autophagic flux (Parkhitko et al., 2011), as indicated by the reduced conversion of LC3-I to the cleaved and lipidated form LC3-II (Fig. 12c). We wondered whether an alteration in the lysosomal route of degradation might explain the YAP accumulation in *Tsc2*^{-/-} MEFs. The lysosomotropic drug and autophagy inhibitor chloroquine (CQ) led to the accumulation of LC3-II that normally undergoes lysosomal turnover. This effect was paralleled by the accumulation of YAP protein in control MEFs, while the amount of YAP was not further increased by chloroquine in *Tsc2*^{-/-} cells (Fig. 12a). In MEFs, YAP protein was localized in cytosol, nucleus and cytosolic vesicles, a fraction of which was also positive for the lysosomal marker Lamp2 (Fig. 12b). Impairment of lysosomal degradation by chloroquine treatment increased the amount of YAP detectable in the lysosomes, indicating that YAP is a cargo for lysosomal degradation. In *Tsc2*^{-/-} cells, the amount of YAP localized in the lysosomes was reduced as compared to control cells in both untreated and chloroquine-treated conditions (Fig. 12b and 12c). Of note, interactome studies in *Drosophila* cells revealed a strong association of the Hippo pathway with endocytosis and vesicle trafficking complexes (Kwon et al., 2013).

To analyze the crosstalk between mTOR kinase activity and YAP, we used torin1, a potent ATP competitive inhibitor of mTOR (Thoreen et al., 2009), as assessed by the dephosphorylation of the mTOR substate 4EBP1 (Fig. 12d and 12e). Torin1 treatment of *Tsc2*^{-/-} MEFs promoted LC3 lipidation, indicating an induction of the autophagic flux, which was accompanied by a reduction of YAP levels (Fig. 12d). The effect of Torin1 was also observed in autophagy competent control MEFs (Fig. 12d and 12e). However, in autophagy deficient *Atg7*^{-/-} MEFs, mTOR inhibition was largely unable to induce YAP degradation (Fig. 12e). Similar to Torin1 treatment, nutrient starvation also promoted YAP degradation concomitantly with the induction of autophagy, in a chloroquine-sensitive manner (Fig. 12f). Of note, ectopic Flag-YAP co-immunoprecipitated with the autophagy cargo receptor p62 and with the upstream kinase Lats1 in basal conditions (Fig. 12g). Upon autophagy induction by nutrient starvation together with chloroquine treatment to induce a late autophagy block, the interaction with p62 and Lats1 was respectively up- and down-regulated. Finally, the *in vivo* deletion of *Atg7* in epithelial cells of kidney proximal tubules was sufficient to cause the accumulation of YAP in lysates from the whole mouse kidneys (Fig. 12h). we extended these observations to two additional models of autophagy deletion in liver: the adenoviral-Cre mediated deletion of *Atg7* in *Atg7*^{f/f} mice and the deletion of

Vps15 in Vps15f/f mice carrying an Albumin-Cre transgene (Vps15f/f; Alb-Cre) (Fig. 13). In conclusion, mTOR regulates YAP degradation through autophagy, which is dependent on ATG7. Our data favour a model in which the control of YAP lysosomal degradation by mTOR matches YAP activity with nutrient availability in growth permissive conditions.

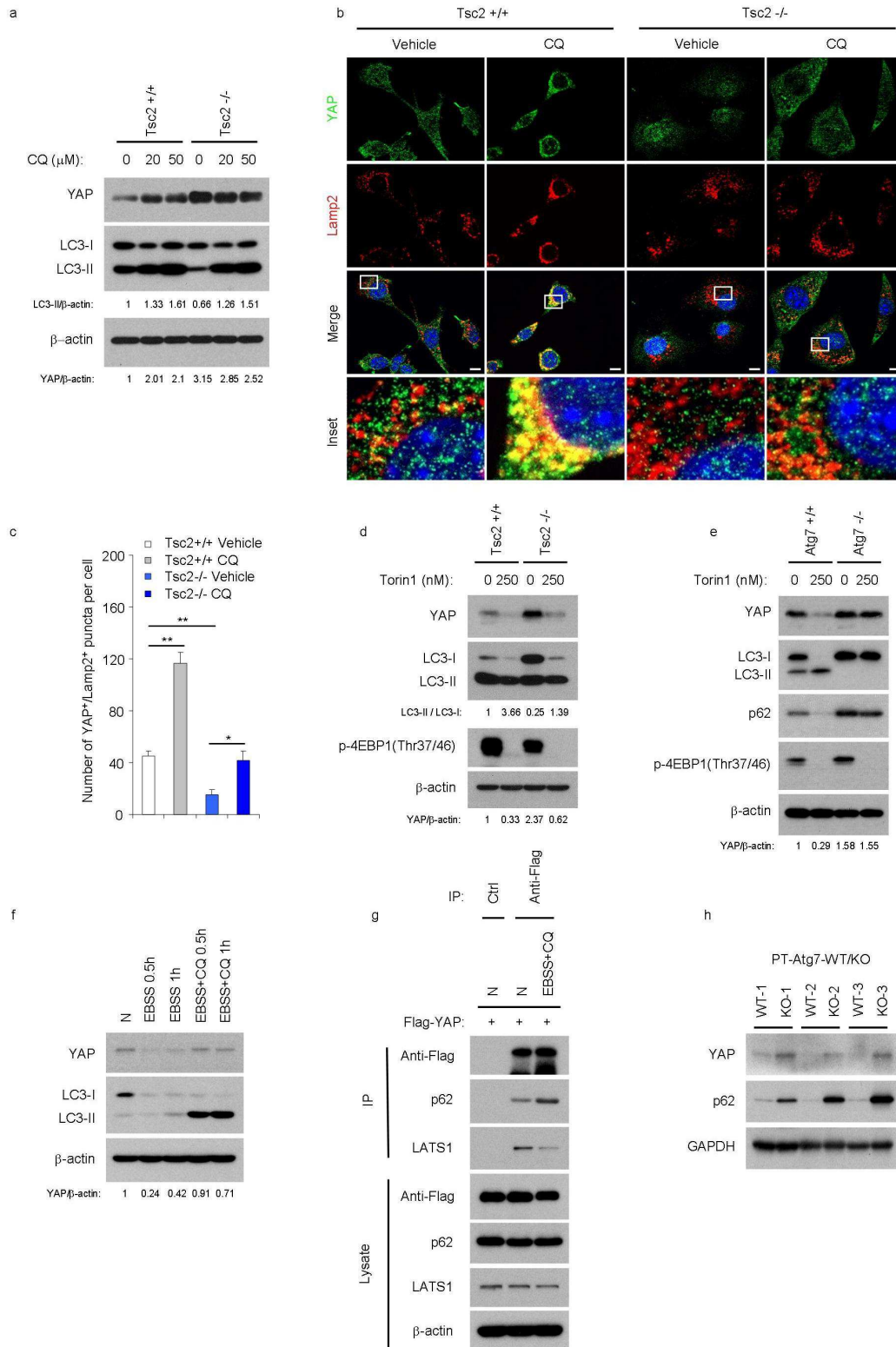


Figure 12. YAP is accumulated in TSC deficient cells due to blockage of autophagy. (a) Expression of indicated proteins was analysed by immunoblot in *Tsc2*^{+/+} and *Tsc2*^{-/-} MEFs treated with or without chloroquine (CQ) for 8 hours. Similar results were observed in three independent experiments. (b, c) Localization of YAP and Lamp2 was analysed by immunofluorescence in *Tsc2*^{+/+} and *Tsc2*^{-/-} MEFs treated with or without CQ (20 μ M) for 24 hours. Insets show part of the cells indicated with squares. 50 cells were counted for yellow punctas in each group. Three independent experiments were performed and analysed (mean \pm s.e.m, * p <0.05, ** p <0.01, Scale bar 10 μ m). (d, e)

Expression of indicated proteins was analysed by immunoblot in *Tsc2*^{+/+}, *Tsc2*^{-/-} and *Atg7*^{+/+}, *Atg7*^{-/-} MEFs culturing with or without Torin1 for 24 hours. Similar results were observed in three independent experiments. (f) Immunoblot analysis of YAP and LC3 in Hela cells with indicated treatments. YAP levels were normalized with β -actin. Similar results were observed in three independent experiments. (g) Immunoprecipitation analysis of interacting proteins of flag-tagged YAP in the indicated culturing conditions for 0.5 hour. Similar results were observed in three independent experiments. (h) Expression of indicated proteins was analysed by immunoblot in ctrl (N=3) and proximal tubules specific *Atg7* knockout mouse kidney samples (N=3).

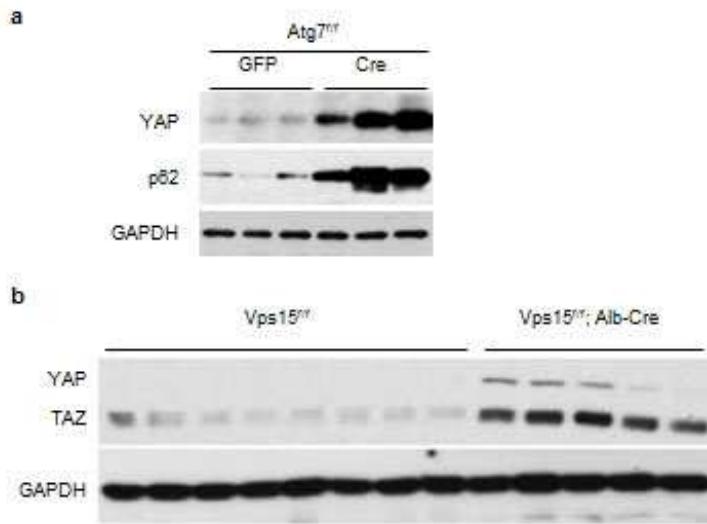


Figure 13. YAP is accumulated in both *Atg7* and *Vps15* deficient livers. (a) Immunoblot analysis of *Atg7*^{f/f} liver extracts two weeks after intravenous injection of Adenoviruses expressing GFP or Cre recombinase. (b) Immunoblot analysis of *Vps15*^{f/f} liver extracts carrying or not the liver specific expression of Cre recombinase.

3 Conclusion and discussion

In this study, we generated a mosaic *Tsc1* mutant mouse model which developed renal mesenchymal lesions showing similarities with human PEComas of TSC patients. To gain insights into the pathogenesis of these lesions, we screened the transcriptional outputs of several signalling pathways, which govern proliferation, differentiation and maintenance of multipotency during development, including Notch, Wnt, Hedgehog and Hippo pathways. Strickingly, we revealed a transcriptional signature of the Hippo pathway in *Tsc1* mutant kidneys. We identified that YAP was upregulated by mTOR in mouse and human TSC1/2 null cells. Inhibition of YAP either genetically or pharmacologically greatly attenuates the abnormal proliferation and induces apoptosis of TSC1/2 null cells, both in vitro and in PEComas of mosaic *Tsc1* mutant mice. Finally, we demonstrated that YAP accumulation in TSC1/2 deficient cells was due to impaired degradation of the protein by autophagy in a mTOR-dependent manner. These results suggested YAP as a potential therapeutical target for TSC and other diseases with dysregulated mTOR activity.

3.1 The cell of origin of TSC-associated PEComas

Utilizing a strategy that targeting *Tsc1* in a portion of cells randomly during development, we were able to reproduce human renal PEComa-like mesenchymal lesions in mice. These two counterparts show similar immunohistochemistry signatures characterized by expression of both myogenic and melanocytic lineage markers. Detailed characterization of this model raised several possibilities to explore the cell of origin of TSC-associated PEComas.

3.1.1 Pericytes

Pericyte is the mural cell of the capillaries which closely associated with endothelial cells contributing to the integrity of small blood vessels. In renal PEComas of *Tsc1* mouse mutant, we observed a small portion of degenerated pericytes labelled by

PDGFR β and α SMA. Intriguingly, pericytes have been shown to be able to differentiate into adipocytes and smooth muscle cells in vitro, which are two major components commonly observed in angiomyolipomas (Armulik et al., 2011). Therefore, disruption of Tsc1/Tsc2 in pericytes specifically should be pursued to explore the possibility of pericytes as the cell of origin of TSC-associated PEComas.

3.1.2 Smooth muscle cells

In the Tsc1 null PEComas, a large portion of cells are α SMA positive or H-caldesmon positive smooth muscle cells. It is possible that they are the prime cell of origin of TSC-associated PEComas. This hypothesis could be test by targeting Tsc1/Tsc2 specifically in smooth muscle cells.

3.1.3 Neural crest cells

Neural Crest is a transient cell population arising during vertebrate development which migrate into multiple organs and differentiate into a diversity of cell types including melanocytes, smooth muscle cells, bone cells, peripheral neurons and glia (Huang and Saint-Jeannet, 2004). Since PEComas express two lineage markers, melanocytic and myogenic markers, It has been proposed that neural crest cells are potential progenitor cells that give rise to PEComas (Lim et al., 2007). It is important to generate TSC mutants using neural crest specific Cre alleles to test this possibility.

3.2 Potential pharmacological strategies against YAP for TSC lesions

We identified that YAP was upregulated in PEComas of Tsc1 mutant mouse models and human PEComas associated with TSC, such as angiomyolipomas and lymphangiomyomatosis. Inhibition of YAP by genetic means or verteporfin, a compound that disrupts the interaction between YAP and its transcription factor

TEAD, greatly suppresses the abnormal proliferation and survival of Tsc1/Tsc2 null cells in vitro and in vivo. These results indicate that YAP is a potential target for TSC therapy and this mouse model can be utilized to test the efficacy of multiple interventions modulating YAP activity for treatment of TSC (Fig. 14).

3.2.1 GPCR agonist/antagonist

A large variety of G protein coupled receptors (GPCR) have been recently identified as positive and negative up-stream regulators of the Hippo/YAP pathway (Yu et al., 2012). Future studies should define the GPCR present in the different TSC lesions and test their activity on YAP. Of note, pharmacological agents acting on the angiotensin and adrenergic GPCR are well tolerated and have interesting actions that should be considered in this scenario. Angiotensin antagonists ameliorate renal injury in conditions of hypertension and fibrosis (Remuzzi et al., 2002). Propranolol, a β adrenergic antagonist, has striking efficacy against infantile hemangioma, possibly due to inhibition of angiogenesis and pericyte functions (Leaute-Labreze et al., 2008). Whether these agents act on YAP and are effective against TSC PEComas, are remarkable possibilities to explore.

3.2.2 Statins

The lipid product of mevalonate pathway, geranylgeranyl pyrophosphate, plays an important role in the post-translational modification of small GTPases, such as Rho and Rheb. Statins, the inhibitors of the rate-limiting enzyme HMG-CoA in the mevalonate pathway which lead to down-regulation of mTOR complex 1 activity through inhibiting Rheb, can also induce YAP/TAZ phosphorylation and nuclear export by acting on Rho GTPase. Interestingly, Simvastatin has already been shown to inhibit the proliferation and survival of TSC2 null cells in vitro, while the efficacy of atorvastatin against TSC remains controversial. Therefore, the effectiveness and molecular mechanism underlying the roles of statins in treating TSC remain to be fully understood.

3.2.3 Peptides inhibiting interaction between YAP and TEAD

The mammalian Vestigial-like proteins VGLL4 have been identified as a transcriptional repressor of YAP through its competitive binding to TEAD1-4 through Tondu domains (Jiao et al., 2014; Zhang et al., 2014a). Peptides mimicking VGLL4's Tondu domains attenuate YAP-dependent tumor growth in vitro and in vivo. It will be interesting to determine the activity of VGLL4 in TSC null cells and test the effect of Tondu domain like peptides in TSC mouse models.

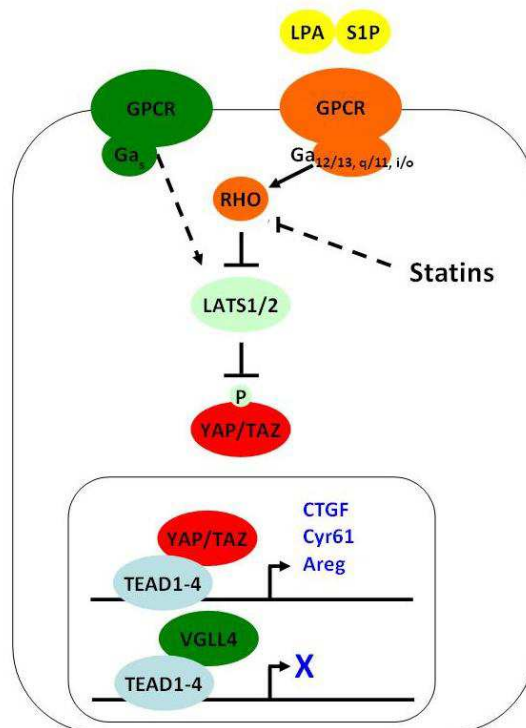


Figure 14. Potential pharmacological strategies against YAP for TSC treatment.

3.3 Regulation of YAP degradation by autophagy

Autophagy is an evolutionally conserved catabolic pathway which recycles cellular proteins and organelles in lysosomes. There are three different forms of autophagy that has been described: macroautophagy, microautophagy and chaperone-mediated autophagy.

Macroautophagy (hereafter as autophagy) sequesters the cellular proteins and damaged organelles in double-membrane autophagosomes, delivers and degrades these cargos in lysosomes. Microautophagy directly engulfs cytosolic cargos like glycogen into lysosomes. Chaperone-mediated autophagy recognizes soluble cargos by chaperone Hsc70, delivers them to the receptor on the lysosomal membrane Lamp2A and translocates the cargos into the lysosomes.

We revealed that YAP protein accumulation in TSC1/2 null cells is due to blockage of macroautophagic degradation of YAP in a mTOR-dependent manner since YAP degradation by inhibition of mTOR is attenuated in ATG7 deficient cells in which autophagosome formation is disrupted. Furthermore, YAP is accumulated in ATG7 deficient renal tubular cells.

There are two ways for the cargos of autophagy, such as proteins or organelles, to be loaded onto double-membrane autophagosomes (Fig. 15). The first route is through directly interacting with ATG8, a protein family that bind to and required for the formation of autophagosomes. The second is by linking targets to ATG8 proteins through cargo receptors, such as p62, NBR1, NDP52, VCP and optineurin (Stolz et al., 2014).

In the future, it is important to identify the responsible cargo receptor that links YAP to autophagosomes and map the precise domain of YAP critical to this interaction. Autophagy is dysregulated in many human diseases such as neurodegeneration disease and cancer and it will be interesting to explore the role of YAP in the pathogenesis of these settings.

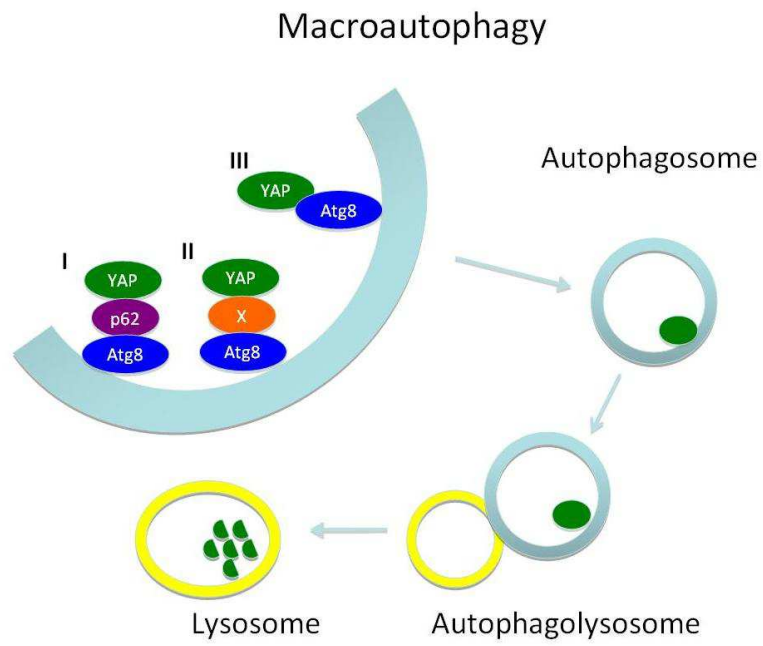


Figure 15. Regulation of YAP degradation through macroautophagy.

4 Materials and Methods

Mice

Tsc1^{fl/fl} and *CAGGCre-ER* mice were obtained from Jackson laboratories. *Yap^{fl/fl}* mice were previously described (Xin et al., 2011). R26-floxstop-LacZ mice were obtained from Dr. Celine Colnot. *Yap^{+/+}* and *Yap^{+/-}* mice were kindly shared by Dr. Udayan Apte. Kidney proximal tubule specific *Atg7* knockout mouse samples, using a modified PEPCCK-driven Cre, were kindly provided by Dr. Zheng Dong. All animal studies were approved by the Direction Départementale des Services Vétérinaires, Prefecture de Police, Paris, France (authorization number 75-1313) and the ethical committee of Paris Descartes University. Mice were housed in a 12-h light/dark cycle and fed a standard chow. All mice used in this study were on mixed genetic background (C57BL/6J, BALB/cJ, or 129/SvJae), with control mice being Cre negative littermates of mutant mice. Female mice were used unless otherwise indicated. Tamoxifen (Sigma) dissolved in corn oil (Sigma) (10 mg/ml) was injected intraperitoneally into pregnant females with a dose of 10 mg/kg at E15.5 (the day of vaginal plug observed was considered as E0.5). 1 mg/ml tamoxifen prepared in corn oil was used to inject subcutaneously the pups (10 mg/kg) at postnatal day 2 to generate mosaic-*Tsc1KO; Yap^{+/-}*. Blood was collected using tubes with EDTA (KABE LABORTECHNIK), centrifuged at 500g for 3mins. Plasma was isolated and analysed for urea levels with Olympus AU400 instrument.

Human TSC samples

Human samples were retrieved from the files of the Department of Pathology and Diagnostics of the University of Verona and from Institut Bergonié of Bordeaux. The frozen samples included five angiomyolipoma samples and two resected kidney samples as consequences of TSC-unrelated diseases, pyelonephritis or oncocytoma. Paraffin embedded human PEComa samples included seven angiomyolipomas, two lymphangiomyomatosis and one hepatic angiomyolipomas. Human studies were ethically approved by the Comité de Protection des Personnes (CPP Ile de France III) with the reference file #AT144.

Cell culture and reagents

HEK293, *Tsc2*^{+/+};*p53*^{-/-} and *Tsc2*^{-/-};*p53*^{-/-} MEFs were cultured in DMEM with 10% FBS, 1% penicillin/streptomycin. *Atg7*^{+/+} and *Atg7*^{-/-} MEFs were kindly provided by Masaaki Komatsu (Komatsu et al., 2005) and cultured in DMEM with 10% FBS, 1% non essential amino acid (Gibco), 1% penicillin/streptomycin. All cells were cultured at 37°C and 5% CO₂. 5 X 10⁴ cells were seeded per well in 6-well plate and cultured overnight before treatment with MG132 (Tocris), Chloroquine (Sigma) or Torin1 (Tocris). For RNAi experiments, 2 X 10⁴ HEK293 cells were seeded per well in 6-well plate, cultured overnight, transfected with siRNAs targeting TSC1, TSC2 and ctrl siRNA (Qiagen) using calcium phosphate method. 48 hours later, second transfection with siRNAs was administered. Cells were harvested 96 hours after the first siRNA transfection. MEFs were transfected with siCtrl and siYAP (Dharmacon) using DharmaFECT1 Transfection Reagent. For nutrient starvation, cells were cultured in EBSS (Gibco) for half an hour or one hour. Flag-YAP plasmid was obtained from Addgene (#19045).

Immunohistochemistry and immunofluorescence

Mouse tissues were fixed in 4% paraformaldehyde, embedded in paraffin and sectioned at 4 μm. Sections were deparaffinized and hydrated before being incubated in citrate buffer (pH6) sub-boiling for 10 mins. Sections were blocked in 3% Goat normal serum, 1% BSA and 0.1% Triton X-100 for one hour and then incubated with the following primary antibodies overnight at 4°C: anti-phospho-rpS6 (#5364), anti-Vimentin (#5741), anti-YAP (#4912), and anti-PDGFRβ (#3169) were from Cell signalling, anti-αSMA (Sigma #A2547), anti-Ki67 (Thermo Scientific #PA5-19462), anti-Pmel/HMB45 (DAKO #M0634), anti-ICAM1 (Santa Cruz #sc-107), anti-H-caldesmon (#ab50016), anti-CD31 (#ab28364), anti-Pmel (#ab137078) and anti-Cathepsin K (#ab19027) were from Abcam. Then sections were incubated with biotinylated secondary antibodies, detected with Vectastain Elite ABC kit (Vector) and DAB chromogen system (DAKO). For immunofluorescence, Alexa488 or Alexa568 conjugated secondary antibodies (Molecular Probe) were used and DNA

was stained by DAPI within the mounting medium (Vector). For immunocytofluorescence, cells were grown on chamber slides (Millipore), fixed in 100% cold methanol, blocked in 3% Goat normal serum, 1% BSA and 0.1% Triton X-100/PBS, and incubated with the following antibodies: anti-YAP (Santa Cruz #sc-101199) and anti-Lamp2 (Abcam #ab13524). Immunofluorescence slides were analysed by microscopy ZEISS ApoTome2. ImageJ software was used for quantification.

Immunoblotting and immunoprecipitation

Cells and tissues were lysed in cell lysis buffer (Cell signalling #9803) with complete protease inhibitor cocktail and phosSTOP phosphatase inhibitor cocktail (Roche). Protein extracts were resolved by SDS-PAGE, transferred to PVDF membranes and incubated with the following primary antibodies: anti- α SMA (Sigma #A2547), anti-Mart1 (Santa Cruz #sc-20032), anti-CTGF (Abcam #ab6992), anti-AREG (Santa Cruz #sc-74501), anti-TSC1 (Invitrogen #37-0400), anti-LC3 (Nano tools #0231-100), anti-p62/SQSTM1 (Abnova #H00008878-M01), anti-GAPDH (Abcam #ab9485), anti- β -actin (Sigma #A5441), anti- α -tubulin (Sigma #T5168), anti-YAP (#4912), anti-YAP/TAZ (#8418), anti-Lamin A/C (#2032), anti-rpS6 (#2217), anti-phospho-rpS6(Ser240/244) (#5364), anti-p4EBP1(Thr37/46) (#2855), anti-pYAP(Ser127) (#4911), anti-Lats1 (#3477), anti-TSC2 (#4308), anti-Ub (#3936) were from Cell signalling. Nuclear and cytoplasmic protein extraction were performed with NE-PER kit (Thermo Scientific #78835). Flag-tagged YAP protein complex was immunoprecipitated from cell lysates with anti-Flag antibody (Sigma #F1804) and protein G sepharose (GE #17-0618-01). Immunocomplexes were washed in cell lysis buffer three times and analysed by immunoblotting.

BrdU labelling

Cells were incubated with BrdU (Sigma) (10 μ g/ml) for three hours before harvest. Then cells were washed, fixed in 4% paraformaldehyde 15 mins, incubated in citrate buffer (pH6) at sub-boiling temperature and detected with an anti-BrdU antibody (Roche #11170376001). The percentage of BrdU incorporation was

determined by counting BrdU-positive nuclei among at least 200 cells in distinct fields. For *in vivo* studies, mice were injected intraperitoneally with BrdU (50 mg/kg) two hours before sacrifice or 24 hours before sacrifice (mosaic-*Tsc1*KO;*Yap*^{+/-} experiments).

TUNEL assay

Terminal deoxyribonucleotidyl transferase-mediated dUTP nick end labelling (TUNEL) assay were performed using In Situ Cell Death Detection Kit (Roche) according to manufacturer's instructions.

Temsirolimus and verteporfin treatments

Temsirolimus (LC Laboratories) was dissolved in 100% ethanol (25 mg/ml), aliquoted and stored at -20°C. 1 mg/ml working solution was prepared in 5% Tween 80, 5% PEG400 and 86% PBS before injection. Mice were injected intraperitoneally with vehicle or temsirolimus (5 mg/kg) every other day for two weeks. Verteporfin (Selleckchem) was dissolved in DMSO (100 mg/ml), aliquoted and stored at -80°C. Working solution was prepared at 10 mg/ml in PBS freshly before use. Mice were administered intraperitoneally with vehicle or verteporfin solution at a dose of 100 mg/kg every other day for ten days. *In vitro*, cells were treated with DMSO or verteporfin with a dose of 4 μM.

Quantitative RT-PCR

Total RNA was extracted from tissue or cells using an RNAeasy Mini Kit (QIAGEN), following manufacturer's instructions. Single-strand cDNA was synthesized from 1 μg of total RNA with SuperScript II (Invitrogen) and random hexamer primers. Real-time quantitative PCR was performed on MX3005P instrument (Agilent) using a Brilliant III SYBR Green QPCR Master Mix (Agilent). Relative amounts of the indicated mRNAs were determined by means of the $2^{-\Delta\Delta CT}$ method, normalizing with β-actin levels. The primer sequences used were mouse β-actin 5'-GTGACGTTGACATCCGTAAAGA-3' and 5'-GCCGGACTCATCGTACTCC-3';

mouse Mart1 5'-TCCCAGGAAGGGGCACAGACG-3' and 5'-
 AGCGTTGGGAACCACGGGCT-3'; mouse Cathepsin K 5'-
 AAGTGGTTCAGAAGATGACGGGAC-3' and 5'-
 TCTTCAGAGTCAATGCCTCCGTTC-3'; mouse Pmel 5'-
 TGACGGTGGACCCTGCCCAT-3' and 5'-AGCTTTGCGTGGCCCGTAGC-3'; mouse
 Tyrp1 5'-CCCTAGCCTATATCTCCCTTTT-3' and 5'-
 TACCATCGTGGGGATAATGGC-3'; mouse Yap 5'-
 GTCCTCCTTTGAGATCCCTGA-3' and 5'-TGTTGTTGTCTGATCGTTGTGAT-3';
 mouse Ctgf 5'-GTGCCAGAACGCACACTG-3' and 5'-CCCCGGTTACACTCCAAA-3';
 mouse Cyr61 5'- GGATCTGTGAAGTGCCTCCT-3' and 5'-
 CTGCATTTCTTGCCCTTTTT-3'; mouse Areg 5'-TCATGGCGAATGCAGATACA-3'
 and 5'-GCTACTACTGCAATCTTGGA-3'; mouse Hes1 5'-
 GGAGAGGCTGCCAAGGTTTT-3' and 5'-GCAAATTGGCCGTCAGGA-3'; mouse
 Hes5 5'-TCTCCACGATGATCCTTAAAGGA-3' and 5'-CAAATCGTGCCACATGC-
 3'; mouse Cdx1 5'- TTCACTACAGCCGGTACATCA-3' and 5'-
 GCCAGCATTAGTAGGGCATAGA-3'; mouse Fgf4 5'-
 TGCCTTTCTTTACCGACGAGT-3' and 5'- GCGTAGGATTCGTAGGCGTT-3'; mouse
 Gli1 5'-CATTCCACAGGACAGCTCAA-3' and 5'-TGGCAGGGCTCTGACTAACT-3';
 mouse Gli2 5'- CCTTCTCCAATGCCTCAGAC-3' and 5'-
 GGGGTCTGTGTACCTCTTGG-3'.

Statistical analysis

Data are shown as means \pm s.e.m. Analysis were performed by unpaired, two-tailed, Student's *t* test unless otherwise indicated. $P < 0.05$ was considered statistically significant.

5 References

Armulik, A., Genove, G., and Betsholtz, C. (2011). Pericytes: developmental, physiological, and pathological perspectives, problems, and promises. *Developmental cell* 21, 193-215.

Astrinidis, A., Cash, T.P., Hunter, D.S., Walker, C.L., Chernoff, J., and Henske, E.P. (2002). Tuberin, the tuberous sclerosis complex 2 tumor suppressor gene product, regulates Rho activation, cell adhesion and migration. *Oncogene* 21, 8470-8476.

Atochina-Vasserman, E.N., Goncharov, D.A., Volgina, A.V., Milavec, M., James, M.L., and Krymskaya, V.P. (2013). Statins in lymphangioliomyomatosis. Simvastatin and atorvastatin induce differential effects on tuberous sclerosis complex 2-null cell growth and signaling. *American journal of respiratory cell and molecular biology* 49, 704-709.

Bar-Peled, L., Chantranupong, L., Cherniack, A.D., Chen, W.W., Ottina, K.A., Grabiner, B.C., Spear, E.D., Carter, S.L., Meyerson, M., and Sabatini, D.M. (2013). A Tumor suppressor complex with GAP activity for the Rag GTPases that signal amino acid sufficiency to mTORC1. *Science* 340, 1100-1106.

Bar-Peled, L., Schweitzer, L.D., Zoncu, R., and Sabatini, D.M. (2012). Ragulator is a GEF for the rag GTPases that signal amino acid levels to mTORC1. *Cell* 150, 1196-1208.

Benvenuto, G., Li, S., Brown, S.J., Braverman, R., Vass, W.C., Cheadle, J.P., Halley, D.J., Sampson, J.R., Wienecke, R., and DeClue, J.E. (2000). The tuberous sclerosis-1 (TSC1) gene product hamartin suppresses cell growth and augments the expression of the TSC2 product tuberin by inhibiting its ubiquitination. *Oncogene* 19, 6306-6316.

Bissler, J.J., Kingswood, J.C., Radzikowska, E., Zonnenberg, B.A., Frost, M., Belousova, E., Sauter, M., Nonomura, N., Brakemeier, S., de Vries, P.J., *et al.* (2013). Everolimus for angiomyolipoma associated with tuberous sclerosis complex or

sporadic lymphangioliomyomatosis (EXIST-2): a multicentre, randomised, double-blind, placebo-controlled trial. *Lancet* 381, 817-824.

Brugarolas, J., Lei, K., Hurley, R.L., Manning, B.D., Reiling, J.H., Hafen, E., Witters, L.A., Ellisen, L.W., and Kaelin, W.G., Jr. (2004). Regulation of mTOR function in response to hypoxia by REDD1 and the TSC1/TSC2 tumor suppressor complex. *Genes & development* 18, 2893-2904.

Byfield, M.P., Murray, J.T., and Backer, J.M. (2005). hVps34 is a nutrient-regulated lipid kinase required for activation of p70 S6 kinase. *The Journal of biological chemistry* 280, 33076-33082.

Cai, S.L., Tee, A.R., Short, J.D., Bergeron, J.M., Kim, J., Shen, J., Guo, R., Johnson, C.L., Kiguchi, K., and Walker, C.L. (2006). Activity of TSC2 is inhibited by AKT-mediated phosphorylation and membrane partitioning. *The Journal of cell biology* 173, 279-289.

Camargo, F.D., Gokhale, S., Johnnidis, J.B., Fu, D., Bell, G.W., Jaenisch, R., and Brummelkamp, T.R. (2007). YAP1 increases organ size and expands undifferentiated progenitor cells. *Current biology : CB* 17, 2054-2060.

Carsillo, T., Astrinidis, A., and Henske, E.P. (2000). Mutations in the tuberous sclerosis complex gene TSC2 are a cause of sporadic pulmonary lymphangioliomyomatosis. *Proceedings of the National Academy of Sciences of the United States of America* 97, 6085-6090.

Chan, S.W., Lim, C.J., Loo, L.S., Chong, Y.F., Huang, C., and Hong, W. (2009). TEADs mediate nuclear retention of TAZ to promote oncogenic transformation. *The Journal of biological chemistry* 284, 14347-14358.

Chen, H.I., Einbond, A., Kwak, S.J., Linn, H., Koepf, E., Peterson, S., Kelly, J.W., and Sudol, M. (1997). Characterization of the WW domain of human yes-associated protein and its polyproline-containing ligands. *The Journal of biological chemistry* 272, 17070-17077.

Corradetti, M.N., Inoki, K., Bardeesy, N., DePinho, R.A., and Guan, K.L. (2004). Regulation of the TSC pathway by LKB1: evidence of a molecular link between

tuberous sclerosis complex and Peutz-Jeghers syndrome. *Genes & development* 18, 1533-1538.

Crino, P.B., Nathanson, K.L., and Henske, E.P. (2006). The tuberous sclerosis complex. *The New England journal of medicine* 355, 1345-1356.

Demetriades, C., Doumpas, N., and Teleman, A.A. (2014). Regulation of TORC1 in response to amino acid starvation via lysosomal recruitment of TSC2. *Cell* 156, 786-799.

Dennis, M.D., Coleman, C.S., Berg, A., Jefferson, L.S., and Kimball, S.R. (2014). REDD1 enhances protein phosphatase 2A-mediated dephosphorylation of Akt to repress mTORC1 signaling. *Science signaling* 7, ra68.

Dibble, C.C., Elis, W., Menon, S., Qin, W., Klekota, J., Asara, J.M., Finan, P.M., Kwiatkowski, D.J., Murphy, L.O., and Manning, B.D. (2012). TBC1D7 is a third subunit of the TSC1-TSC2 complex upstream of mTORC1. *Molecular cell* 47, 535-546.

Dong, J., Feldmann, G., Huang, J., Wu, S., Zhang, N., Comerford, S.A., Gayyed, M.F., Anders, R.A., Maitra, A., and Pan, D. (2007). Elucidation of a universal size-control mechanism in *Drosophila* and mammals. *Cell* 130, 1120-1133.

Dupont, S., Morsut, L., Aragona, M., Enzo, E., Giulitti, S., Cordenonsi, M., Zanconato, F., Le Digabel, J., Forcato, M., Bicciato, S., *et al.* (2011). Role of YAP/TAZ in mechanotransduction. *Nature* 474, 179-183.

El-Hashemite, N., Zhang, H., Henske, E.P., and Kwiatkowski, D.J. (2003). Mutation in TSC2 and activation of mammalian target of rapamycin signalling pathway in renal angiomyolipoma. *Lancet* 361, 1348-1349.

Fan, R., Kim, N.G., and Gumbiner, B.M. (2013). Regulation of Hippo pathway by mitogenic growth factors via phosphoinositide 3-kinase and phosphoinositide-dependent kinase-1. *Proceedings of the National Academy of Sciences of the United States of America* 110, 2569-2574.

Fernandez, B.G., Gaspar, P., Bras-Pereira, C., Jezowska, B., Rebelo, S.R., and Janody, F. (2011). Actin-Capping Protein and the Hippo pathway regulate F-actin and tissue growth in *Drosophila*. *Development* 138, 2337-2346.

Findlay, G.M., Yan, L., Procter, J., Mieulet, V., and Lamb, R.F. (2007). A MAP4 kinase related to Ste20 is a nutrient-sensitive regulator of mTOR signalling. *The Biochemical journal* 403, 13-20.

Franz, D.N. (2013). Everolimus in the treatment of subependymal giant cell astrocytomas, angiomyolipomas, and pulmonary and skin lesions associated with tuberous sclerosis complex. *Biologics : targets & therapy* 7, 211-221.

Ganem, N.J., Cornils, H., Chiu, S.Y., O'Rourke, K.P., Arnaud, J., Yimlamai, D., They, M., Camargo, F.D., and Pellman, D. (2014). Cytokinesis failure triggers hippo tumor suppressor pathway activation. *Cell* 158, 833-848.

Gao, X., Neufeld, T.P., and Pan, D. (2000). *Drosophila* PTEN regulates cell growth and proliferation through PI3K-dependent and -independent pathways. *Developmental biology* 221, 404-418.

Gao, X., and Pan, D. (2001). TSC1 and TSC2 tumor suppressors antagonize insulin signaling in cell growth. *Genes & development* 15, 1383-1392.

Gao, X., Zhang, Y., Arrazola, P., Hino, O., Kobayashi, T., Yeung, R.S., Ru, B., and Pan, D. (2002). Tsc tumour suppressor proteins antagonize amino-acid-TOR signalling. *Nature cell biology* 4, 699-704.

Goberdhan, D.C., Paricio, N., Goodman, E.C., Mlodzik, M., and Wilson, C. (1999). *Drosophila* tumor suppressor PTEN controls cell size and number by antagonizing the Chico/PI3-kinase signaling pathway. *Genes & development* 13, 3244-3258.

Goto, J., Talos, D.M., Klein, P., Qin, W., Chekaluk, Y.I., Anderl, S., Malinowska, I.A., Di Nardo, A., Bronson, R.T., Chan, J.A., *et al.* (2011). Regulable neural progenitor-specific Tsc1 loss yields giant cells with organellar dysfunction in a model of tuberous sclerosis complex. *Proceedings of the National Academy of Sciences of the United States of America* 108, E1070-1079.

Halder, G., and Johnson, R.L. (2011). Hippo signaling: growth control and beyond. *Development* 138, 9-22.

Hossain, Z., Ali, S.M., Ko, H.L., Xu, J., Ng, C.P., Guo, K., Qi, Z., Ponniah, S., Hong, W., and Hunziker, W. (2007). Glomerulocystic kidney disease in mice with a targeted inactivation of *Wwtr1*. *Proceedings of the National Academy of Sciences of the United States of America* 104, 1631-1636.

Huang, H., Potter, C.J., Tao, W., Li, D.M., Brogiolo, W., Hafen, E., Sun, H., and Xu, T. (1999). PTEN affects cell size, cell proliferation and apoptosis during *Drosophila* eye development. *Development* 126, 5365-5372.

Huang, J., Dibble, C.C., Matsuzaki, M., and Manning, B.D. (2008). The TSC1-TSC2 complex is required for proper activation of mTOR complex 2. *Molecular and cellular biology* 28, 4104-4115.

Huang, J., and Manning, B.D. (2008). The TSC1-TSC2 complex: a molecular switchboard controlling cell growth. *The Biochemical journal* 412, 179-190.

Huang, X., and Saint-Jeannet, J.P. (2004). Induction of the neural crest and the opportunities of life on the edge. *Developmental biology* 275, 1-11.

Inoki, K., Li, Y., Xu, T., and Guan, K.L. (2003). Rheb GTPase is a direct target of TSC2 GAP activity and regulates mTOR signaling. *Genes & development* 17, 1829-1834.

Inoki, K., Li, Y., Zhu, T., Wu, J., and Guan, K.L. (2002). TSC2 is phosphorylated and inhibited by Akt and suppresses mTOR signalling. *Nature cell biology* 4, 648-657.

Inoki, K., Ouyang, H., Zhu, T., Lindvall, C., Wang, Y., Zhang, X., Yang, Q., Bennett, C., Harada, Y., Stankunas, K., *et al.* (2006). TSC2 integrates Wnt and energy signals via a coordinated phosphorylation by AMPK and GSK3 to regulate cell growth. *Cell* 126, 955-968.

Jiao, S., Wang, H., Shi, Z., Dong, A., Zhang, W., Song, X., He, F., Wang, Y., Zhang, Z., Wang, W., *et al.* (2014). A peptide mimicking VGLL4 function acts as a YAP antagonist therapy against gastric cancer. *Cancer cell* 25, 166-180.

Jin, F., Wienecke, R., Xiao, G.H., Maize, J.C., Jr., DeClue, J.E., and Yeung, R.S. (1996). Suppression of tumorigenicity by the wild-type tuberous sclerosis 2 (Tsc2) gene and its C-terminal region. *Proceedings of the National Academy of Sciences of the United States of America* 93, 9154-9159.

Kandt, R.S., Haines, J.L., Smith, M., Northrup, H., Gardner, R.J., Short, M.P., Dumars, K., Roach, E.S., Steingold, S., Wall, S., *et al.* (1992). Linkage of an important gene locus for tuberous sclerosis to a chromosome 16 marker for polycystic kidney disease. *Nature genetics* 2, 37-41.

Karbowniczek, M., Yu, J., and Henske, E.P. (2003). Renal angiomyolipomas from patients with sporadic lymphangiomyomatosis contain both neoplastic and non-neoplastic vascular structures. *The American journal of pathology* 162, 491-500.

Kenerson, H.L., Aicher, L.D., True, L.D., and Yeung, R.S. (2002). Activated mammalian target of rapamycin pathway in the pathogenesis of tuberous sclerosis complex renal tumors. *Cancer research* 62, 5645-5650.

Kim, S., Kim, S.F., Maag, D., Maxwell, M.J., Resnick, A.C., Juluri, K.R., Chakraborty, A., Koldobskiy, M.A., Cha, S.H., Barrow, R., *et al.* (2011). Amino acid signaling to mTOR mediated by inositol polyphosphate multikinase. *Cell metabolism* 13, 215-221.

Knudson, A.G., Jr. (1971). Mutation and cancer: statistical study of retinoblastoma. *Proceedings of the National Academy of Sciences of the United States of America* 68, 820-823.

Kobayashi, T., Minowa, O., Kuno, J., Mitani, H., Hino, O., and Noda, T. (1999). Renal carcinogenesis, hepatic hemangiomas, and embryonic lethality caused by a germ-line Tsc2 mutation in mice. *Cancer research* 59, 1206-1211.

Kobayashi, T., Minowa, O., Sugitani, Y., Takai, S., Mitani, H., Kobayashi, E., Noda, T., and Hino, O. (2001). A germ-line Tsc1 mutation causes tumor development and embryonic lethality that are similar, but not identical to, those caused by Tsc2 mutation in mice. *Proceedings of the National Academy of Sciences of the United States of America* 98, 8762-8767.

Kwiatkowski, D.J., Zhang, H., Bandura, J.L., Heiberger, K.M., Glogauer, M., el-Hashemite, N., and Onda, H. (2002). A mouse model of TSC1 reveals sex-dependent lethality from liver hemangiomas, and up-regulation of p70S6 kinase activity in Tsc1 null cells. *Human molecular genetics* 11, 525-534.

Kwon, Y., Vinayagam, A., Sun, X., Dephore, N., Gygi, S.P., Hong, P., and Perrimon, N. (2013). The Hippo signaling pathway interactome. *Science* 342, 737-740.

Lamb, R.F., Roy, C., Diefenbach, T.J., Vinters, H.V., Johnson, M.W., Jay, D.G., and Hall, A. (2000). The TSC1 tumour suppressor hamartin regulates cell adhesion through ERM proteins and the GTPase Rho. *Nature cell biology* 2, 281-287.

Laplane, M., and Sabatini, D.M. (2012). mTOR signaling in growth control and disease. *Cell* 149, 274-293.

Lee, D.F., Kuo, H.P., Chen, C.T., Hsu, J.M., Chou, C.K., Wei, Y., Sun, H.L., Li, L.Y., Ping, B., Huang, W.C., *et al.* (2007). IKK beta suppression of TSC1 links inflammation and tumor angiogenesis via the mTOR pathway. *Cell* 130, 440-455.

Lim, S.D., Stallcup, W., Lefkove, B., Govindarajan, B., Au, K.S., Northrup, H., Lang, D., Fisher, D.E., Patel, A., Amin, M.B., *et al.* (2007). Expression of the neural stem cell markers NG2 and L1 in human angiomyolipoma: are angiomyolipomas neoplasms of stem cells? *Molecular medicine* 13, 160-165.

Liu-Chittenden, Y., Huang, B., Shim, J.S., Chen, Q., Lee, S.J., Anders, R.A., Liu, J.O., and Pan, D. (2012). Genetic and pharmacological disruption of the TEAD-YAP complex suppresses the oncogenic activity of YAP. *Genes & development* 26, 1300-1305.

Long, X., Lin, Y., Ortiz-Vega, S., Yonezawa, K., and Avruch, J. (2005). Rheb binds and regulates the mTOR kinase. *Current biology : CB* 15, 702-713.

Magri, L., Cambiaghi, M., Cominelli, M., Alfaro-Cervello, C., Cursi, M., Pala, M., Bulfone, A., Garcia-Verdugo, J.M., Leocani, L., Minicucci, F., *et al.* (2011). Sustained activation of mTOR pathway in embryonic neural stem cells leads to development of tuberous sclerosis complex-associated lesions. *Cell stem cell* 9, 447-462.

Mak, B.C., Kenerson, H.L., Aicher, L.D., Barnes, E.A., and Yeung, R.S. (2005). Aberrant beta-catenin signaling in tuberous sclerosis. *The American journal of pathology* 167, 107-116.

Malhowski, A.J., Hira, H., Bashiruddin, S., Warburton, R., Goto, J., Robert, B., Kwiatkowski, D.J., and Finlay, G.A. (2011). Smooth muscle protein-22-mediated deletion of Tsc1 results in cardiac hypertrophy that is mTORC1-mediated and reversed by rapamycin. *Human molecular genetics* 20, 1290-1305.

Martignoni, G., Pea, M., Reghellin, D., Zamboni, G., and Bonetti, F. (2008). PEComas: the past, the present and the future. *Virchows Archiv : an international journal of pathology* 452, 119-132.

Matsumoto, S., Bandyopadhyay, A., Kwiatkowski, D.J., Maitra, U., and Matsumoto, T. (2002). Role of the Tsc1-Tsc2 complex in signaling and transport across the cell membrane in the fission yeast *Schizosaccharomyces pombe*. *Genetics* 161, 1053-1063.

Meikle, L., Talos, D.M., Onda, H., Pollizzi, K., Rotenberg, A., Sahin, M., Jensen, F.E., and Kwiatkowski, D.J. (2007). A mouse model of tuberous sclerosis: neuronal loss of Tsc1 causes dysplastic and ectopic neurons, reduced myelination, seizure activity, and limited survival. *The Journal of neuroscience : the official journal of the Society for Neuroscience* 27, 5546-5558.

Menon, S., Dibble, C.C., Talbott, G., Hoxhaj, G., Valvezan, A.J., Takahashi, H., Cantley, L.C., and Manning, B.D. (2014). Spatial control of the TSC complex integrates insulin and nutrient regulation of mTORC1 at the lysosome. *Cell* 156, 771-785.

Miller, E., Yang, J., DeRan, M., Wu, C., Su, A.I., Bonamy, G.M., Liu, J., Peters, E.C., and Wu, X. (2012). Identification of serum-derived sphingosine-1-phosphate as a small molecule regulator of YAP. *Chemistry & biology* 19, 955-962.

Morin-Kensicki, E.M., Boone, B.N., Howell, M., Stonebraker, J.R., Teed, J., Alb, J.G., Magnuson, T.R., O'Neal, W., and Milgram, S.L. (2006). Defects in yolk sac vasculogenesis, chorioallantoic fusion, and embryonic axis elongation in mice with targeted disruption of Yap65. *Molecular and cellular biology* 26, 77-87.

Oka, T., Remue, E., Meerschaert, K., Vanloo, B., Boucherie, C., Gfeller, D., Bader, G.D., Sidhu, S.S., Vandekerckhove, J., Gettemans, J., *et al.* (2010). Functional complexes between YAP2 and ZO-2 are PDZ domain-dependent, and regulate YAP2 nuclear localization and signalling. *The Biochemical journal* 432, 461-472.

Onda, H., Lueck, A., Marks, P.W., Warren, H.B., and Kwiatkowski, D.J. (1999). *Tsc2(+/-)* mice develop tumors in multiple sites that express gelsolin and are influenced by genetic background. *The Journal of clinical investigation* 104, 687-695.

Ota, M., and Sasaki, H. (2008). Mammalian Tead proteins regulate cell proliferation and contact inhibition as transcriptional mediators of Hippo signaling. *Development* 135, 4059-4069.

Pan, D. (2010). The hippo signaling pathway in development and cancer. *Developmental cell* 19, 491-505.

Parkhitko, A., Myachina, F., Morrison, T.A., Hindi, K.M., Auricchio, N., Karbowniczek, M., Wu, J.J., Finkel, T., Kwiatkowski, D.J., Yu, J.J., *et al.* (2011). Tumorigenesis in tuberous sclerosis complex is autophagy and p62/sequestosome 1 (SQSTM1)-dependent. *Proceedings of the National Academy of Sciences of the United States of America* 108, 12455-12460.

Pea, M., Martignoni, G., Zamboni, G., and Bonetti, F. (1996). Perivascular epithelioid cell. *The American journal of surgical pathology* 20, 1149-1153.

Peterson, T.R., Sengupta, S.S., Harris, T.E., Carmack, A.E., Kang, S.A., Balderas, E., Guertin, D.A., Madden, K.L., Carpenter, A.E., Finck, B.N., *et al.* (2011). mTOR complex 1 regulates lipin 1 localization to control the SREBP pathway. *Cell* 146, 408-420.

Plank, T.L., Yeung, R.S., and Henske, E.P. (1998). Hamartin, the product of the tuberous sclerosis 1 (TSC1) gene, interacts with tuberlin and appears to be localized to cytoplasmic vesicles. *Cancer research* 58, 4766-4770.

Poon, C.L., Zhang, X., Lin, J.I., Manning, S.A., and Harvey, K.F. (2012). Homeodomain-interacting protein kinase regulates Hippo pathway-dependent tissue growth. *Current biology : CB* 22, 1587-1594.

Potter, C.J., Huang, H., and Xu, T. (2001). *Drosophila* Tsc1 functions with Tsc2 to antagonize insulin signaling in regulating cell growth, cell proliferation, and organ size. *Cell* 105, 357-368.

Roux, P.P., Ballif, B.A., Anjum, R., Gygi, S.P., and Blenis, J. (2004). Tumor-promoting phorbol esters and activated Ras inactivate the tuberous sclerosis tumor suppressor complex via p90 ribosomal S6 kinase. *Proceedings of the National Academy of Sciences of the United States of America* 101, 13489-13494.

Sancak, Y., Bar-Peled, L., Zoncu, R., Markhard, A.L., Nada, S., and Sabatini, D.M. (2010). Regulator-Rag complex targets mTORC1 to the lysosomal surface and is necessary for its activation by amino acids. *Cell* 141, 290-303.

Sancak, Y., Peterson, T.R., Shaul, Y.D., Lindquist, R.A., Thoreen, C.C., Bar-Peled, L., and Sabatini, D.M. (2008). The Rag GTPases bind raptor and mediate amino acid signaling to mTORC1. *Science* 320, 1496-1501.

Sansores-Garcia, L., Bossuyt, W., Wada, K., Yonemura, S., Tao, C., Sasaki, H., and Halder, G. (2011). Modulating F-actin organization induces organ growth by affecting the Hippo pathway. *The EMBO journal* 30, 2325-2335.

Sarnat, H.B., and Flores-Sarnat, L. (2005). Embryology of the neural crest: its inductive role in the neurocutaneous syndromes. *Journal of child neurology* 20, 637-643.

Schlegelmilch, K., Mohseni, M., Kirak, O., Pruszek, J., Rodriguez, J.R., Zhou, D., Kreger, B.T., Vasioukhin, V., Avruch, J., Brummelkamp, T.R., *et al.* (2011). Yap1 acts downstream of alpha-catenin to control epidermal proliferation. *Cell* 144, 782-795.

Sepp, T., Yates, J.R., and Green, A.J. (1996). Loss of heterozygosity in tuberous sclerosis hamartomas. *Journal of medical genetics* 33, 962-964.

Settembre, C., Zoncu, R., Medina, D.L., Vetrini, F., Erdin, S., Erdin, S., Huynh, T., Ferron, M., Karsenty, G., Vellard, M.C., *et al.* (2012). A lysosome-to-nucleus signalling mechanism senses and regulates the lysosome via mTOR and TFEB. *The EMBO journal* 31, 1095-1108.

Shaw, R.J., Bardeesy, N., Manning, B.D., Lopez, L., Kosmatka, M., DePinho, R.A., and Cantley, L.C. (2004). The LKB1 tumor suppressor negatively regulates mTOR signaling. *Cancer cell* 6, 91-99.

Sidor, C.M., Brain, R., and Thompson, B.J. (2013). Mask proteins are cofactors of Yorkie/YAP in the Hippo pathway. *Current biology* : CB 23, 223-228.

Smith, E.M., Finn, S.G., Tee, A.R., Browne, G.J., and Proud, C.G. (2005). The tuberous sclerosis protein TSC2 is not required for the regulation of the mammalian target of rapamycin by amino acids and certain cellular stresses. *The Journal of biological chemistry* 280, 18717-18727.

Stocker, H., and Hafen, E. (2000). Genetic control of cell size. *Current opinion in genetics & development* 10, 529-535.

Stocker, H., Radimerski, T., Schindelholz, B., Wittwer, F., Belawat, P., Daram, P., Breuer, S., Thomas, G., and Hafen, E. (2003). Rheb is an essential regulator of S6K in controlling cell growth in *Drosophila*. *Nature cell biology* 5, 559-565.

Stolz, A., Ernst, A., and Dikic, I. (2014). Cargo recognition and trafficking in selective autophagy. *Nature cell biology* 16, 495-501.

Strano, S., Munarriz, E., Rossi, M., Castagnoli, L., Shaul, Y., Sacchi, A., Oren, M., Sudol, M., Cesareni, G., and Blandino, G. (2001). Physical interaction with Yes-associated protein enhances p73 transcriptional activity. *The Journal of biological chemistry* 276, 15164-15173.

Strassburger, K., Tiebe, M., Pinna, F., Breuhahn, K., and Teleman, A.A. (2012). Insulin/IGF signaling drives cell proliferation in part via Yorkie/YAP. *Developmental biology* 367, 187-196.

Tapon, N., and Harvey, K.F. (2012). The Hippo pathway--from top to bottom and everything in between. *Seminars in cell & developmental biology* 23, 768-769.

Tapon, N., Ito, N., Dickson, B.J., Treisman, J.E., and Hariharan, I.K. (2001). The *Drosophila* tuberous sclerosis complex gene homologs restrict cell growth and cell proliferation. *Cell* 105, 345-355.

Tsai, P.T., Hull, C., Chu, Y., Greene-Colozzi, E., Sadowski, A.R., Leech, J.M., Steinberg, J., Crawley, J.N., Regehr, W.G., and Sahin, M. (2012). Autistic-like behaviour and cerebellar dysfunction in Purkinje cell Tsc1 mutant mice. *Nature* 488, 647-651.

Tumaneng, K., Russell, R.C., and Guan, K.L. (2012a). Organ size control by Hippo and TOR pathways. *Current biology : CB* 22, R368-379.

Tumaneng, K., Schlegelmilch, K., Russell, R.C., Yimlamai, D., Basnet, H., Mahadevan, N., Fitamant, J., Bardeesy, N., Camargo, F.D., and Guan, K.L. (2012b). YAP mediates crosstalk between the Hippo and PI(3)K-TOR pathways by suppressing PTEN via miR-29. *Nature cell biology* 14, 1322-1329.

Uhlmann, E.J., Wong, M., Baldwin, R.L., Bajenaru, M.L., Onda, H., Kwiatkowski, D.J., Yamada, K., and Gutmann, D.H. (2002). Astrocyte-specific TSC1 conditional knockout mice exhibit abnormal neuronal organization and seizures. *Annals of neurology* 52, 285-296.

van Slegtenhorst, M., de Hoogt, R., Hermans, C., Nellist, M., Janssen, B., Verhoef, S., Lindhout, D., van den Ouweland, A., Halley, D., Young, J., *et al.* (1997). Identification of the tuberous sclerosis gene TSC1 on chromosome 9q34. *Science* 277, 805-808.

van Slegtenhorst, M., Nellist, M., Nagelkerken, B., Cheadle, J., Snell, R., van den Ouweland, A., Reuser, A., Sampson, J., Halley, D., and van der Sluijs, P. (1998). Interaction between hamartin and tuberlin, the TSC1 and TSC2 gene products. *Human molecular genetics* 7, 1053-1057.

Vassilev, A., Kaneko, K.J., Shu, H., Zhao, Y., and DePamphilis, M.L. (2001). TEAD/TEF transcription factors utilize the activation domain of YAP65, a Src/Yes-associated protein localized in the cytoplasm. *Genes & development* 15, 1229-1241.

Wada, K., Itoga, K., Okano, T., Yonemura, S., and Sasaki, H. (2011). Hippo pathway regulation by cell morphology and stress fibers. *Development* 138, 3907-3914.

Wang, Y., Dong, Q., Zhang, Q., Li, Z., Wang, E., and Qiu, X. (2010). Overexpression of yes-associated protein contributes to progression and poor prognosis of non-small-cell lung cancer. *Cancer science* 101, 1279-1285.

Wienecke, R., Konig, A., and DeClue, J.E. (1995). Identification of tuberin, the tuberous sclerosis-2 product. Tuberin possesses specific Rap1GAP activity. *The Journal of biological chemistry* 270, 16409-16414.

Xiao, G.H., Shoarinejad, F., Jin, F., Golemis, E.A., and Yeung, R.S. (1997). The tuberous sclerosis 2 gene product, tuberin, functions as a Rab5 GTPase activating protein (GAP) in modulating endocytosis. *The Journal of biological chemistry* 272, 6097-6100.

Xie, Z., and Klionsky, D.J. (2007). Autophagosome formation: core machinery and adaptations. *Nature cell biology* 9, 1102-1109.

Xin, M., Kim, Y., Sutherland, L.B., Qi, X., McAnally, J., Schwartz, R.J., Richardson, J.A., Bassel-Duby, R., and Olson, E.N. (2011). Regulation of insulin-like growth factor signaling by Yap governs cardiomyocyte proliferation and embryonic heart size. *Science signaling* 4, ra70.

Xu, M.Z., Yao, T.J., Lee, N.P., Ng, I.O., Chan, Y.T., Zender, L., Lowe, S.W., Poon, R.T., and Luk, J.M. (2009). Yes-associated protein is an independent prognostic marker in hepatocellular carcinoma. *Cancer* 115, 4576-4585.

Yagi, R., Chen, L.F., Shigesada, K., Murakami, Y., and Ito, Y. (1999). A WW domain-containing yes-associated protein (YAP) is a novel transcriptional co-activator. *The EMBO journal* 18, 2551-2562.

Yu, F.X., and Guan, K.L. (2013). The Hippo pathway: regulators and regulations. *Genes & development* 27, 355-371.

Yu, F.X., Zhao, B., Panupinthu, N., Jewell, J.L., Lian, I., Wang, L.H., Zhao, J., Yuan, H., Tumaneng, K., Li, H., *et al.* (2012). Regulation of the Hippo-YAP pathway by G-protein-coupled receptor signaling. *Cell* 150, 780-791.

Zhang, H., Cicchetti, G., Onda, H., Koon, H.B., Asrican, K., Bajraszewski, N., Vazquez, F., Carpenter, C.L., and Kwiatkowski, D.J. (2003). Loss of Tsc1/Tsc2 activates mTOR and disrupts PI3K-Akt signaling through downregulation of PDGFR. *The Journal of clinical investigation* 112, 1223-1233.

Zhang, L., Ye, D.X., Pan, H.Y., Wei, K.J., Wang, L.Z., Wang, X.D., Shen, G.F., and Zhang, Z.Y. (2011). Yes-associated protein promotes cell proliferation by activating Fos Related Activator-1 in oral squamous cell carcinoma. *Oral oncology* 47, 693-697.

Zhang, W., Gao, Y., Li, P., Shi, Z., Guo, T., Li, F., Han, X., Feng, Y., Zheng, C., Wang, Z., *et al.* (2014a). VGLL4 functions as a new tumor suppressor in lung cancer by negatively regulating the YAP-TEAD transcriptional complex. *Cell research* 24, 331-343.

Zhang, X., Milton, C.C., Humbert, P.O., and Harvey, K.F. (2009). Transcriptional output of the Salvador/warts/hippo pathway is controlled in distinct fashions in *Drosophila melanogaster* and mammalian cell lines. *Cancer research* 69, 6033-6041.

Zhang, Y., Nicholatos, J., Dreier, J.R., Ricoult, S.J., Widenmaier, S.B., Hotamisligil, G.S., Kwiatkowski, D.J., and Manning, B.D. (2014b). Coordinated regulation of protein synthesis and degradation by mTORC1. *Nature*.

Zhao, B., Li, L., Lu, Q., Wang, L.H., Liu, C.Y., Lei, Q., and Guan, K.L. (2011). Angiomotin is a novel Hippo pathway component that inhibits YAP oncoprotein. *Genes & development* 25, 51-63.

Zhao, B., Li, L., Tumaneng, K., Wang, C.Y., and Guan, K.L. (2010). A coordinated phosphorylation by Lats and CK1 regulates YAP stability through SCF(beta-TRCP). *Genes & development* 24, 72-85.

Zhao, B., Wei, X., Li, W., Udan, R.S., Yang, Q., Kim, J., Xie, J., Ikenoue, T., Yu, J., Li, L., *et al.* (2007). Inactivation of YAP oncoprotein by the Hippo pathway is involved in cell contact inhibition and tissue growth control. *Genes & development* 21, 2747-2761.

Zhao, B., Ye, X., Yu, J., Li, L., Li, W., Li, S., Yu, J., Lin, J.D., Wang, C.Y., Chinnaiyan, A.M., *et al.* (2008). TEAD mediates YAP-dependent gene induction and growth control. *Genes & development* 22, 1962-1971.

Zhou, J., Brugarolas, J., and Parada, L.F. (2009). Loss of Tsc1, but not Pten, in renal tubular cells causes polycystic kidney disease by activating mTORC1. *Human molecular genetics* 18, 4428-4441.

Zhou, J., Shrikhande, G., Xu, J., McKay, R.M., Burns, D.K., Johnson, J.E., and Parada, L.F. (2011). Tsc1 mutant neural stem/progenitor cells exhibit migration deficits and give rise to subependymal lesions in the lateral ventricle. *Genes & development* 25, 1595-1600.

Zoncu, R., Bar-Peled, L., Efeyan, A., Wang, S., Sancak, Y., and Sabatini, D.M. (2011). mTORC1 senses lysosomal amino acids through an inside-out mechanism that requires the vacuolar H(+)-ATPase. *Science* 334, 678-683.

6 Publication

Liang N., Zhang C., Dill P., Panasyuk G., Pion D., Koka V., Gallazzini M., Olson E., Lam H., Henske E.P., Dong Z., Apte U., Pallet N., Johnson R., Terzi F., Kwiatkowski D.J., Scoazec J., Martignoni G., **Pende M.** 2014. Regulation of YAP by mTOR and autophagy reveals a therapeutic target of Tuberous Sclerosis Complex. *The Journal of experimental medicine*, 211 (11), 2249-2263.

7 Acknowledgements

I appreciate the supervision and guidance from my mentor Mario Pende throughout these four-year PhD studies. He taught me how to design experiments and how to analyse data. He trained me the way of performing scientific investigation, step by step logically and confidently. He showed me how to deliver a scientific speech and how to construct and describe an intriguing science story in words. I cannot forget his open, critical and constructive attitudes during our discussion on research progress nearly every other day. His grand scientific vision, collaborative and working-hard spirits lighten my future path to become a scientist. His much guidance and help during these four years provide me an opportunity to start an attractive scientific career. Thanks a lot, Mario!

I would like to thank Chi Zhang, with whom I worked side by side during the last two years of my PhD and characterized the role of YAP in TSC-associated PEComas together. I want to thank Ganna Panasyuk, Caroline Treins and Ivan Nemazanyy who taught me how to work with mice and multiple experimental techniques especially in my orientation year. I appreciate the much help from Vonda Koka and Delphine Pion who provided me a lot of significant and helpful technical support. I thank Yves De Keyzer, Stephanie Puget, Patricia Dill, Gregory Bonfils, Cecilia Patitucci, Karim Nadra, Catherine Caillaud and Laura Rouviere for their helpful scientific suggestions. And I would like to thank Prof. Fabiola Terzi, Prof. Guido Martignoni, Prof. David J. Kwiatkowski and Prof. Stefano Fumagalli for their insightful comments and constructive help to this study.

Finally, I would like to thank my wife Shu Zhang and our lovely baby Yacheng who provided me with warm supports to finish this study. I appreciate the strong support from my parents, families and friends whom I missed a lot during my PhD studies in Paris.